

**NASA  
Technical  
Paper  
2195**

August 1983

# Temperature Distribution in an Aircraft Tire at Low Ground Speeds

**John Locke McCarty  
and John A. Tanner**

NASA  
TP  
2195  
c.1



**LOAN COPY: RETURN TO  
AFWL TECHNICAL LIBRARY  
KIRTLAND AFB, NM 87117**



25th Anniversary  
1958-1983



**NASA  
Technical  
Paper  
2195**

1983

# **Temperature Distribution in an Aircraft Tire at Low Ground Speeds**

**John Locke McCarty  
and John A. Tanner**  
*Langley Research Center  
Hampton, Virginia*

**NASA**  
National Aeronautics  
and Space Administration  
**Scientific and Technical  
Information Branch**

1983



## SUMMARY

An experimental study was conducted to define temperature profiles of 22 x 5.5, type VII, bias ply aircraft tires subjected to freely rolling, yawed rolling, and light braking conditions. Results of this investigation indicate that temperatures along the inner wall of the freely rolling tires were greater than those near the outer surface. The effect of increasing tire deflection was to increase the temperature within the shoulder and sidewall areas of the tire carcass. The effect of cornering and braking was to increase the tread temperature. For taxi operations at fixed yaw angles, the temperature profiles were not symmetric. Increasing the ground speed produced only moderate increases in tread temperature, whereas the temperatures in the carcass shoulder and sidewall were essentially unaffected.

## INTRODUCTION

Because of the transient nature of their service requirements, aircraft tires operate under substantially heavier loadings and greater deflections than tires for other vehicles. Typically, an aircraft tire must carry a large load for a relatively short period of time during both takeoff and landing, and the heat generated within the tire during these operations is normally allowed to dissipate prior to the next use cycle. With this design philosophy, an aircraft tire can carry far greater loads than those that would normally be carried in continuous service where the temperature buildup must be controlled due to long-term material strength and fatigue limitations. This philosophy has obviously been a good one as evidenced by the thousands of aircraft tires currently in satisfactory service. A major shortcoming of this design philosophy, however, is that it can be overextended to allow temperatures to build up to dangerous levels which may damage the materials involved (cord-rubber matrix) and eventually lead to tire failure. One condition which can precipitate such a failure is the lengthy taxi distances required at some airports between the terminal and the runway. During these long taxi runs prior to takeoff the tire can generate considerable heat which may be coupled with high tire stresses since the aircraft is operating at its heaviest load. A similar tire temperature/stress condition develops when one tire on a dual or a dual-tandem landing gear fails thereby overloading the remaining tire(s) on the same gear. This condition is discussed in detail in reference 1. In another scenario, temperatures may be just high enough to cause a slow heat degradation to take place and render the tire unfit for the multiple retreading normally done on aircraft tires.

Generally, tires are designed for the loading stresses and, because of the lack of available data, little or no allowance is made for the reduction in structural integrity due to the interaction of stress and temperature. Available automobile and truck tire temperature data are reviewed in reference 2 where it is pointed out that many tire properties (for example, fatigue life, tread wear, and speed potential) are adversely affected by high temperature, and heat is considered to be the great enemy of tires. It is further stated in reference 2 that attention must be directed toward minimizing heat generation, avoiding its concentration in particular zones, and using materials which maintain required properties at the attained temperatures. Heat generation and heat resistance are the responsibility of rubber compounders and textile scientists, whereas heat concentration is mostly determined by tire design (ref. 2). Thus a need exists to study the complex nature of the interaction of

stress and temperature during all ground operational phases of an aircraft tire. To meet this need, a research program was initiated by NASA to predict and measure the temperature distribution within an aircraft tire to aid in defining the strength and fatigue limitations of the tire carcass structure.

The purpose of this paper is to present results from an experimental study to define temperature profiles in the carcass of a tire undergoing free rolling, light braking, and yawed rolling conditions. Data from this study are being used to support development of an analytical method for predicting tire temperature distribution. Analytical and limited experimental effort is underway at the University of Michigan under a NASA Grant and some results of that effort are presented in references 3 and 4.

#### SYMBOLS

Values are given in both SI and U.S. Customary Units. The measurements and calculations were made in U.S. Customary Units. Factors relating the two systems are given in reference 5.

d	rolling distance
T	tire carcass temperature
V	ground speed
$\delta$	tire vertical deflection
$\psi$	yaw angle

#### APPARATUS AND TEST PROCEDURE

##### Tires and Thermocouple Installation

The tires of this investigation were size 22 x 5.5, 12-ply rating, type VII, bias ply aircraft tires which were instrumented with thermocouples and retreaded with a standard rubber stock. Most of the thermocouple installation was done by implanting the sensors in holes drilled into the tire carcass after the carcasses had been buffed prior to retreading. All tires were cured in the same mold; thus, all tires had the same tread pattern of four circumferential grooves similar to that illustrated in the cross-sectional sketch of figure 1. The purpose of this figure is to identify the approximate physical location of the 18 thermocouples which were installed to define the carcass temperature distribution. The 18 thermocouples were mounted on the inner and outer walls of the tires and along an approximate midline at six stations labeled A through F. These thermocouple locations were selected to permit studies of the temperature distribution both through the thickness of the carcass as well as around the meridian of the cross section. The inside thermocouple at each station is referred to as being in row 1, the midline thermocouple in row 2, and the thermocouple on the outer wall is considered in row 3. Thus, the thermocouple identified as station C, row 3 is that which is along the outer wall of the tire and, as the figure shows, in the tire shoulder area.

## Ground Test Vehicle and Instrumentation

A photograph of the ground test vehicle employed in this investigation is shown as figure 2 and the tire test fixture with key components identified is shown in figure 3. A close-up of a tire showing the thermocouple connections through the slip ring assembly is shown in figure 4. Vertical load was applied to the tire by means of two pneumatic cylinders and this load, together with the drag load on the tire during braking tests, was measured by strain-gage beams in the tire test fixture. Most of the tests involved a free rolling tire; however, several tests entailed operating the tire at fixed slip ratios to simulate braking and others involved yawing the tire to duplicate cornering. For the fixed-slip-ratio tests, the tire was driven through a universal coupling by gears which were chain driven by a driving wheel on the vehicle. This operation is described in more detail in reference 6. For the yaw tests, the entire fixture was rotated to the preselected yaw angle and clamped in place.

The output from the carcass thermocouples, as collected through slip rings, was recorded as the printout from a data logger which periodically sampled the multiple thermocouple channels and converted the information to engineering (temperature) units. The instrumented trailing wheel, seen in figures 2 and 3, provided an accurate measurement of speed and distance to the vehicle operator and this information plus the outputs from the strain-gage beams were recorded on an oscillograph.

### Test Technique

The testing technique involved driving the ground vehicle at the desired test speed the length of an approximately 2743 m (9000 ft) asphalt runway at the Wallops Flight Center while monitoring the temperatures and loadings sensed by the instrumented test tire in addition to the vehicle speed and distance. Data were acquired with the tire freely rolling, yawed rolling, and at fixed slip ratios to simulate braked rolling conditions. The tire was tested at deflections of 25, 30, and 35 percent which bracket the nominal aircraft tire operational deflection of 32 percent. For these tests, the tire was loaded to a nominal 18 kN (4000 lb) and the inflation pressure was adjusted to yield the desired deflections. Those inflation pressures were 0.86, 0.67, and 0.50 MPa (125, 97, and 73 psi). To simulate aircraft taxi conditions, all testing was conducted at a nominal ground speed of 32 km/hr (20 mph) except for one series where the speed range was increased to 80 km/hr (50 mph).

Whether the tire was free rolling, yawed, or braked, the test procedure remained the same. The vehicle was first positioned at one end of the runway and the test tire lowered to the surface and loaded to 18 kN (4000 lb). The vehicle was then rapidly accelerated to 32 km/hr (20 mph) and driven the length of the runway at that speed. The oscillograph, which recorded all data except the outputs from the thermocouples, was switched on prior to the tire loading operation and remained on until the test was completed and the loading removed. The data logger was engaged when the vehicle commenced to roll and, while keyed to the oscillograph, provided a temperature printout from all 18 thermocouples every 10 seconds throughout the test run.

For the unyawed free rolling and the fixed slip ratio tests, it was assumed that the temperature distribution was symmetrical about the tire center line (only one side of each test tire was equipped with thermocouples) and only one test run was necessary to define the temperature buildup in the tire carcass for each test condition. However, for the yawed rolling tests, it was necessary to conduct each run

twice with the tire yawed both clockwise and counterclockwise to obtain temperature data on both sides of the tire and thus complete the temperature profile picture. For such repeat runs, the tire was cooled between runs by spraying it with cool water until the thermocouples registered temperatures which closely approximated initial values.

Testing of a particular tire was concluded when thermocouple-wire failures became excessive or, in the case of the yawed and braked tests, when approximately half the tread rubber had been removed due to scrubbing in the tire footprint.

## RESULTS AND DISCUSSION

The growth in tire carcass temperatures with distance traveled is typified by the data of figure 5. These temperatures were obtained from the data logger print-outs of the thermocouple responses which, in a few cases, necessitated some, but not extensive, fairing because of obvious erratic thermocouple behavior during the course of a run. In other situations, the temperature data are limited because of failures to individual thermocouples. The data are presented on a row-by-row basis to illustrate temperature variations from crown to bead along the inside, midline, and outside of the tire cross section. As expected, tire carcass temperatures increase with distance traveled and the rate of increase varies throughout the carcass. (See fig. 5.)

The effect on the temperature distribution in a tire carcass due to extended roll distance, tire deflection, yaw angle, slip ratio, and ground speed is examined in some detail in the following paragraphs. The examination compares temperature levels at corresponding thermocouple locations for each variable after the test tire had traveled a specified distance during a run. Comparisons are made on the basis of the temperature distribution both around the meridian of the tire cross section at three carcass depths (rows 1, 2, and 3) and through the thickness of the tire carcass at various meridional locations (stations A through F). In addition, sketches are included to illustrate visually the differences in the temperature profiles.

### Effect of Extended Roll Distance

As noted in figure 5, test distances for obtaining uninterrupted temperature data were limited by the length of the 2.7 km (1.7 miles) runway. Those distances never exceeded approximately 2.5 km (1.5 miles) since the remaining runway length was needed to decelerate the vehicle from its 32 km/hr (20 mph) test speed. A review of the data indicated that all temperatures increased with distance but that the rate at which the temperatures increased generally became less with distance traveled. This trend suggested that the tire carcass was approaching an equilibrium temperature profile, and many passes were made in both directions on the test runway at 32 km/hr (20 mph) to establish this profile. It became apparent after the tire had traveled approximately 19 812 m (65 000 ft) that each thermocouple was approaching an equilibrium value. The final temperature profile, obtained after 24 384 m (80 000 ft), is presented in figure 6 and shows temperatures approaching 149°C (300°F) near the shoulder area (station C) in figure 6(a). It is clearly illustrated in figure 6(b) that temperatures along the inner wall (row 1) of the sidewall region from shoulder to bead (stations C to F), are considerably greater than those near the outer surface (row 3). The center-line tread temperature (station A, row 3) is somewhat lower than that in the adjacent tread area (station B, row 3). Lower center-line temperatures were also observed from tread surface temperature measurements made with a hand-held pyrometer immediately following the tests.

These lower center-line tread temperatures suggest that there is less tread scrubbing along the center line than along the adjacent tread stations and this trend may be a function of the bias-ply construction of the tire. These lower center-line temperatures may also be influenced by footprint bearing pressure distributions, which tend to be lower along the tread center line than at other tread locations (ref. 7).

A sketch illustrating the complete temperature profile for the extended roll test condition is presented in figure 6(c). The equilibrium temperature of the tire inner wall from station B to station E is above 121°C (250°F) which can lead to premature tire failures (ref. 2). The temperature contour lines in this sketch and all subsequent temperature profile sketches represent a hand fairing of the thermocouple data.

Equilibrium temperatures in automotive and truck tires have been recorded over higher test speeds in references 2 and 7, among others, generally by inserting thermocouple needles into the tire after lengthy test runs. As anticipated, equilibrium temperatures are shown to increase consistently with increasing speed.

#### Effect of Tire Deflection

To explore the influence of tire deflection on temperature buildup in the carcass, a series of tests were run with a free rolling tire, a braked tire, and a yawed tire, each at various deflection values. For these tests the different deflections were obtained by changing the tire inflation pressure while maintaining the nominal 18 kN (4000 lb) vertical loading. The results of those tests are discussed in the paragraphs which follow.

Free rolling tire.- The data of figure 7 illustrate the effect of tire deflection on the distribution of temperature within the tire carcass after the tire had rolled freely for a distance of 1524 m (5000 ft). Data are lacking in the tread region (stations A and B), but similar tests on other tires showed little effect of tire deflection on temperatures in that area. All data show little difference in temperatures between deflections of 25 and 30 percent but a significant increase in temperature results when the deflection is extended to 35 percent.

Aircraft tires are designed to operate at vertical deflections ranging up to 32 percent and these results indicate that taxi operations at greater deflections can lead to significantly higher tire temperatures. In figure 7(c), this temperature increase is more pronounced along the inner surface of the tire sidewall and shoulder, and it is attributed to the more severe sidewall flexing associated with the increased tire deflection.

Braked tire.- The effect of tire deflection on temperature buildup in the carcass of a tire in the braking mode is illustrated in figure 8. The temperature data of this figure were acquired after the tire had traveled 1524 m (5000 ft) at a nominal slip ratio of 10 percent and at deflections of 25, 30, and 35 percent of the tire cross section. The braking effort was simulated by the test truck driving mechanism and the test wheel was not equipped with a brake. The data in the figure indicate that the temperature levels generally increase with increasing tire vertical deflection and these temperature increases are more pronounced in the tread and shoulder area. These results again suggest that the increased tire temperatures are induced by the increased carcass flexing associated with higher tire deflections.



Yawed tire.- Differences in temperature buildup due to changes in the deflection of a yawed tire are presented in figure 9. Data are provided for a tire operating at a yaw angle of 6° and deflected 25 and 35 percent of its cross-sectional height. The comparison is made after the tire had traveled a distance of 2134 m (7000 ft). The tire temperature data for the entire carcass cross section are presented in figures 9(a) and (b) to illustrate the loss of symmetry in the temperature profile due to the yaw angle, and the temperature contour sketches are shown in figure 9(c). The temperatures in the tire sidewall and shoulder tend to be greater for the higher vertical deflections as expected, but along the carcass midline (row 2) in the vicinity of the tread, the opposite trend was observed.

Summary.- Increasing tire vertical deflections generally increases the temperature of the tire carcass regardless of the test condition. For the free rolling and yawed tire tests these temperature increases are more prominent in the tire shoulder and sidewall areas. For the braked tire test the temperature increase is more pronounced in the tread and shoulder areas. For each test, the temperature increases are associated with the increased carcass flexing associated with the higher tire deflections.

#### Effect of Yaw Angle

The effect of yaw angle on the distribution of temperature in a tire carcass is best illustrated in figure 10 where data acquired at yaw angles of 0°, 3°, and 6° are presented after the tire had traveled a distance of 2134 m (7000 ft). Again, the temperature data for the entire carcass cross section are presented in figures 10(a) and (b) to illustrate the loss of symmetry as the yaw angle increases, and the temperature contour sketches are presented in figure 10(c). These data are plotted such that the direction of the cornering force is to the right. A study of these figures shows a substantial temperature rise with increasing yaw angle in the tread area. These elevated tread temperatures are more pronounced along the carcass midline (row 2) and outer surface (row 3) than along the inner wall (row 1). This result suggests that the higher tread temperatures are due to the increased scrubbing action in the tire footprint associated with the increasing yaw angle. The loss of symmetry in the temperature profile, which is associated with increasing yaw angle, is more pronounced along the carcass inner wall. This asymmetry is characterized by elevated temperatures in the right-hand shoulder and sidewall areas of the tire carcass and by slightly reduced temperatures in the left-hand shoulder and sidewall areas as the yaw angle is increased from zero. These trends indicate that the right-hand side of the tire carcass is subjected to greater flexing as the yaw angle increases and the left-hand side of the tire is subjected to reduced flexing.

#### Effect of Slip Ratio

The effect of slip ratio on tire temperature distribution is illustrated by the data of figure 11 taken from tests at nominal slip ratios of 0, 0.05, and 0.10 after the tire in each test had traveled a distance of 2134 m (7000 ft). The drag force friction coefficients for the braking tests were computed to be 0.29 and 0.49 for slip ratios of 0.05 and 0.10, respectively. It should again be emphasized that the braking action was simulated by the driving mechanism of the test truck and no brake was installed in the test wheel. Thus the tire bead and sidewall areas were not subjected to brake heating effects and the data presented in figure 11 depict the thermal effects associated with the braking energy dissipated by the tire. It is

readily apparent from the figure that increased slip ratios increase tire temperatures in the tread area and this buildup is greatest at or near the outer surface.

#### Effect of Speed

To obtain some indication of the influence of taxi speed on trends in tire temperature growth, a series of test runs were made at speed ranges from 32 km/hr (20 mph) to 80 km/hr (50 mph). The temperature distributions after the tire had traveled 2134 m (7000 ft) at the different test speeds are presented in figure 12. The figure suggests that the effect of wheel speed is small. The sidewall temperature is essentially unaffected and only moderate increases of about 30°C (54°F) are noted in the tread temperature as the speed is increased, at least within the speed range examined. The rise in tread temperature at higher speeds is perhaps the result of the higher frequency squirming action which has been observed in the tire footprint. Figure 12(b) further illustrates a trend typical of most test results reported herein. In general the interior carcass temperatures are higher than the outer edge temperatures along the tire shoulder, sidewall, and bead and the outer edge temperatures are higher than the interior temperatures in the tread area. These trends suggest that the primary heat source for the shoulder, sidewall, and bead areas is associated with the damping characteristics of the tire materials and the primary heat source for the tread area is associated with the generation of friction forces in the contact region.

#### CONCLUDING REMARKS

An experimental study was conducted to define the temperature profiles in the carcass of 22 x 5.5, type VII, bias ply aircraft tires subjected to freely rolling, yawed rolling, and light braking conditions. The tires were instrumented with thermocouples implanted in the carcass during a retreading process. The braking tests consisted of gearing the tire to a driving wheel of a ground vehicle to provide operations at fixed slip ratios on a dry runway surface. The cornering tests involved freely rolling the tire at fixed yaw angles up to 6°.

The results from this investigation indicate that the temperatures along the inner wall of the freely rolling tires were greater than those near the outer surface. The effect of increasing the tire deflection was to increase the temperature within the shoulder and sidewall areas of the tire carcass. The effect of cornering (yaw angle effects) and braking (slip ratio effects) was to increase the tire tread temperature. For taxi operations at fixed yaw angles the temperature profiles were not symmetric. Increasing the ground speed produced only moderate increases in the tread temperature, whereas the tire sidewall temperatures were essentially unaffected. Finally, the trends observed in this study suggest that the primary heat source for the tire shoulder, sidewall, and bead areas is associated with the damping characteristics of the tire materials and the primary heat source for the tread area is associated with the generation of friction forces in the contact region.

Langley Research Center  
National Aeronautics and Space Administration  
Hampton, VA 23665  
July 5, 1983

#### REFERENCES

1. Durup, Paul C.: Improvement of Overload Capability of Air Carrier Aircraft Tires. Rep. No. FAA-RD-78-133, Oct. 1978.
2. Conant, F. S.: Tire Temperatures. Rubber Chem. Technol., vol. 44, no. 2, 1971, pp. 397-439.
3. Clark, Samuel K.; and Dodge, Richard N.: Heat Generation in Aircraft Tires Under Free Rolling Conditions. NASA CR-3629, 1982.
4. Dodge, Richard N.; and Clark, Samuel K.: Recent Aircraft Tire Thermal Studies. SAE Tech. Paper Series 821392, Oct. 1982.
5. Standard for Metric Practice. E 380-79, American Soc. Testing & Mater., c.1980.
6. McCarty, John L.; Yager, Thomas J.; and Riccitiello, S. R.: Wear, Friction, and Temperature Characteristics of an Aircraft Tire Undergoing Braking and Cornering. NASA TP-1569, 1979.
7. Clark, Samuel K., ed.: Mechanics of Pneumatic Tires. U.S. Dep. Transp., 1981.

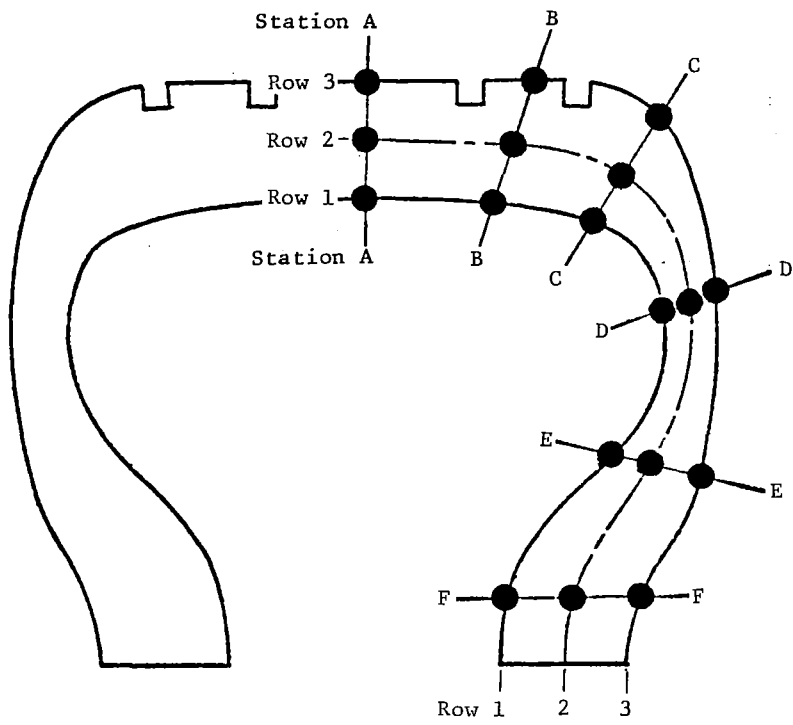


Figure 1.- Thermocouple identification and location in tire carcass.

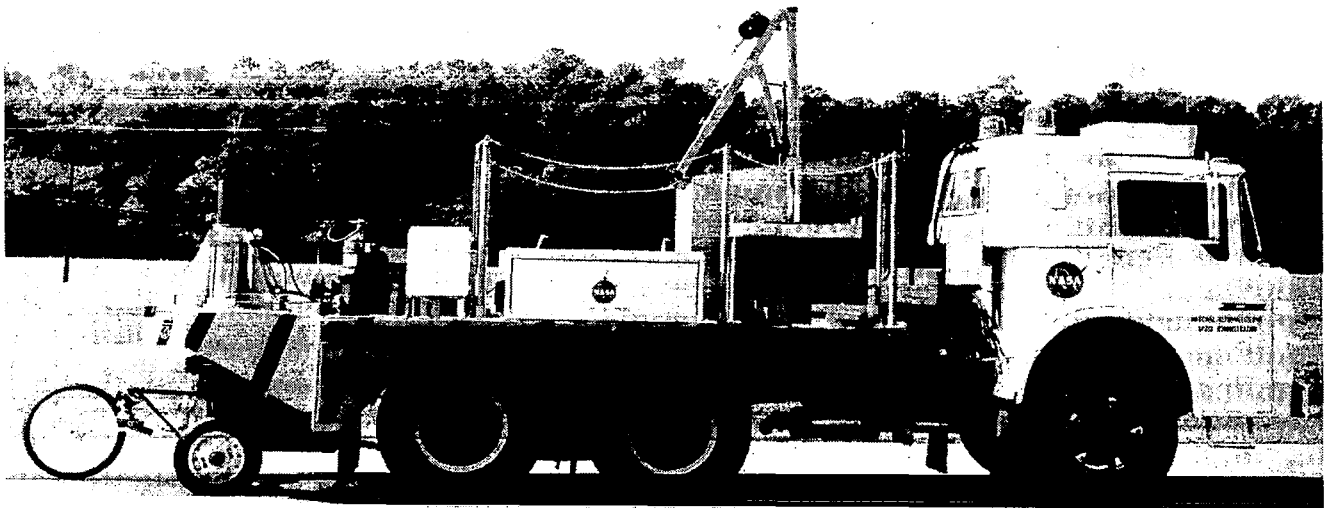


Figure 2.- Ground test vehicle.

L-83-95

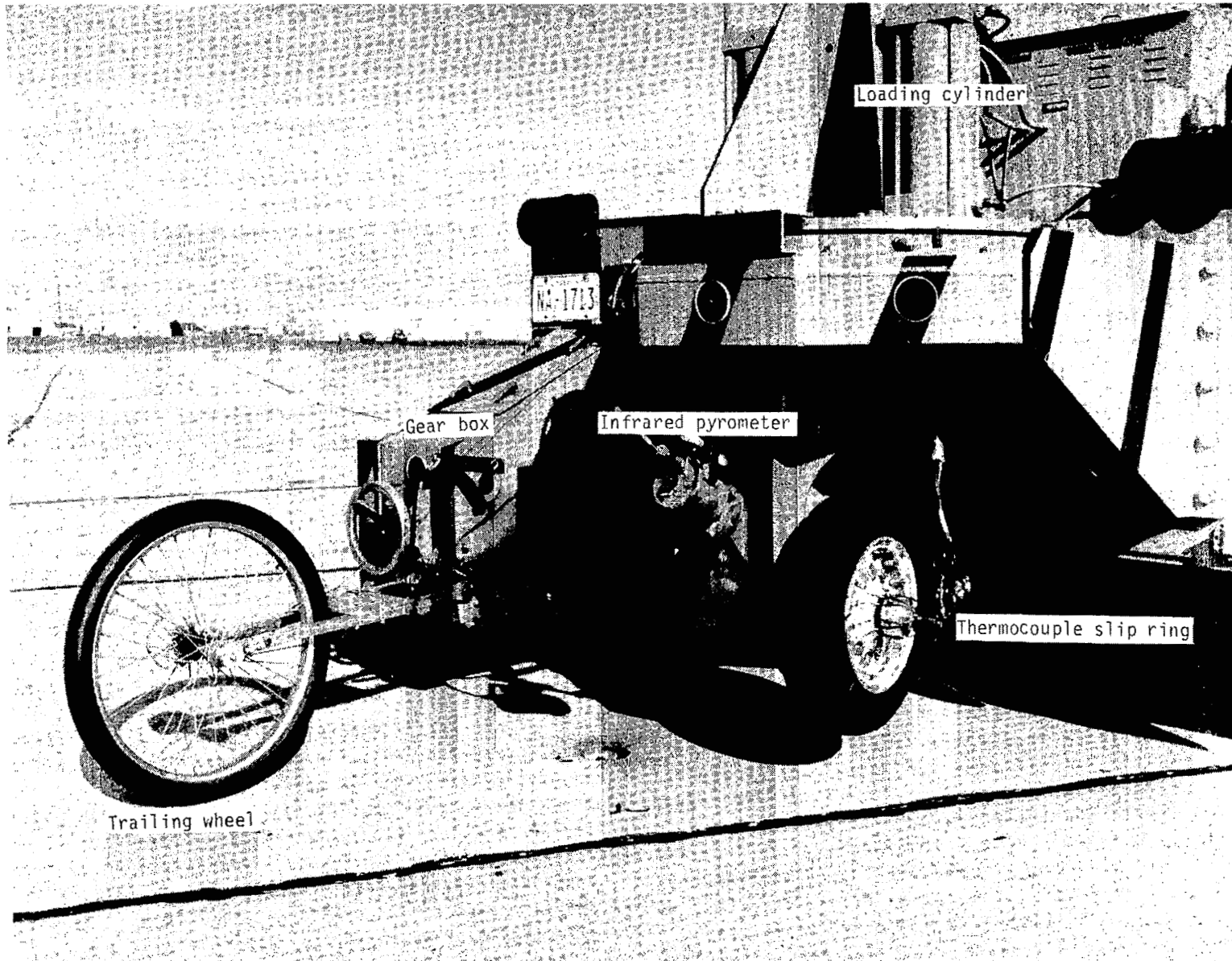
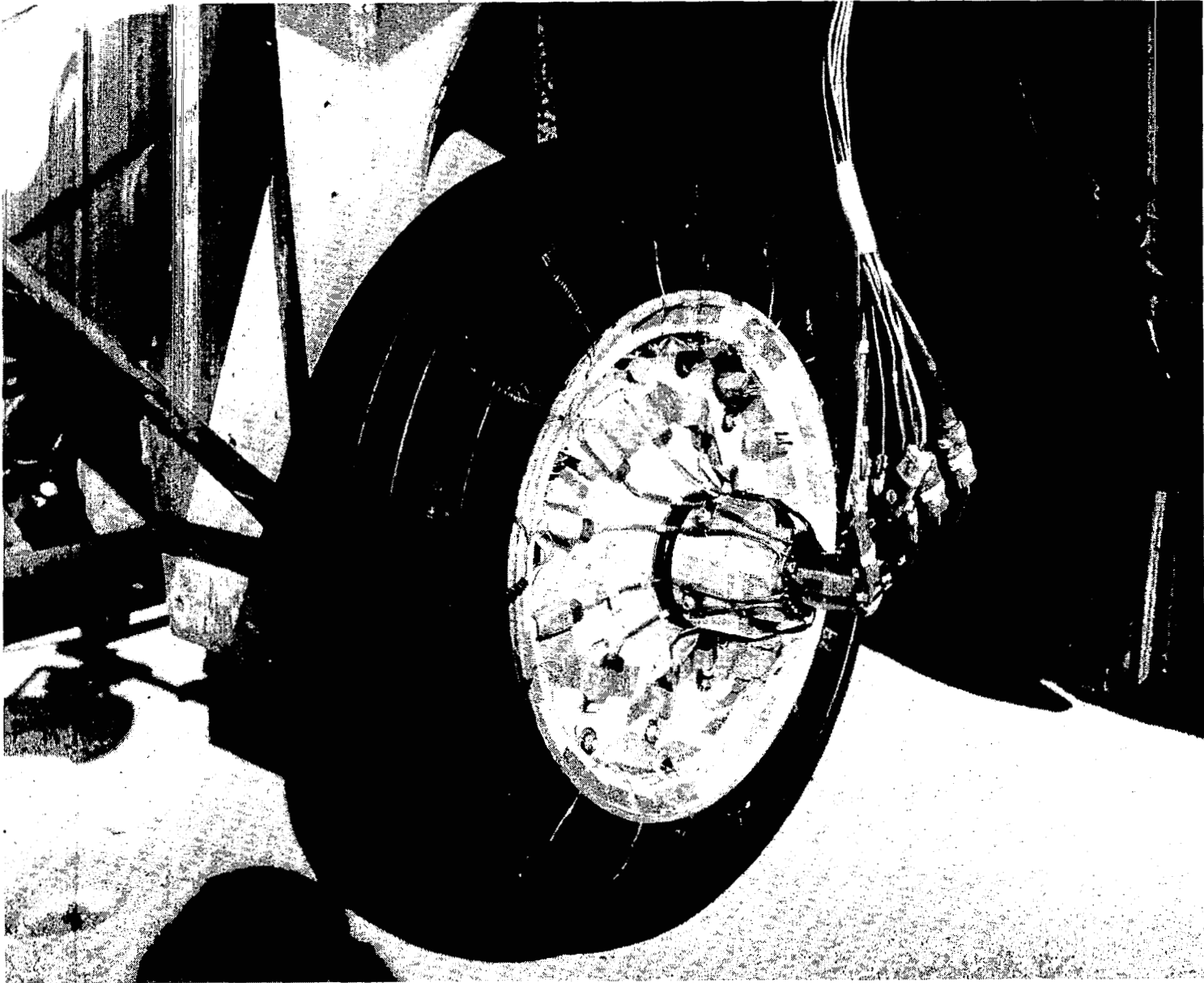


Figure 3.- Tire test fixture showing major components.

L-83-96



L-83-97

Figure 4.- Close-up of test tire showing thermocouple connections through slip ring assembly.

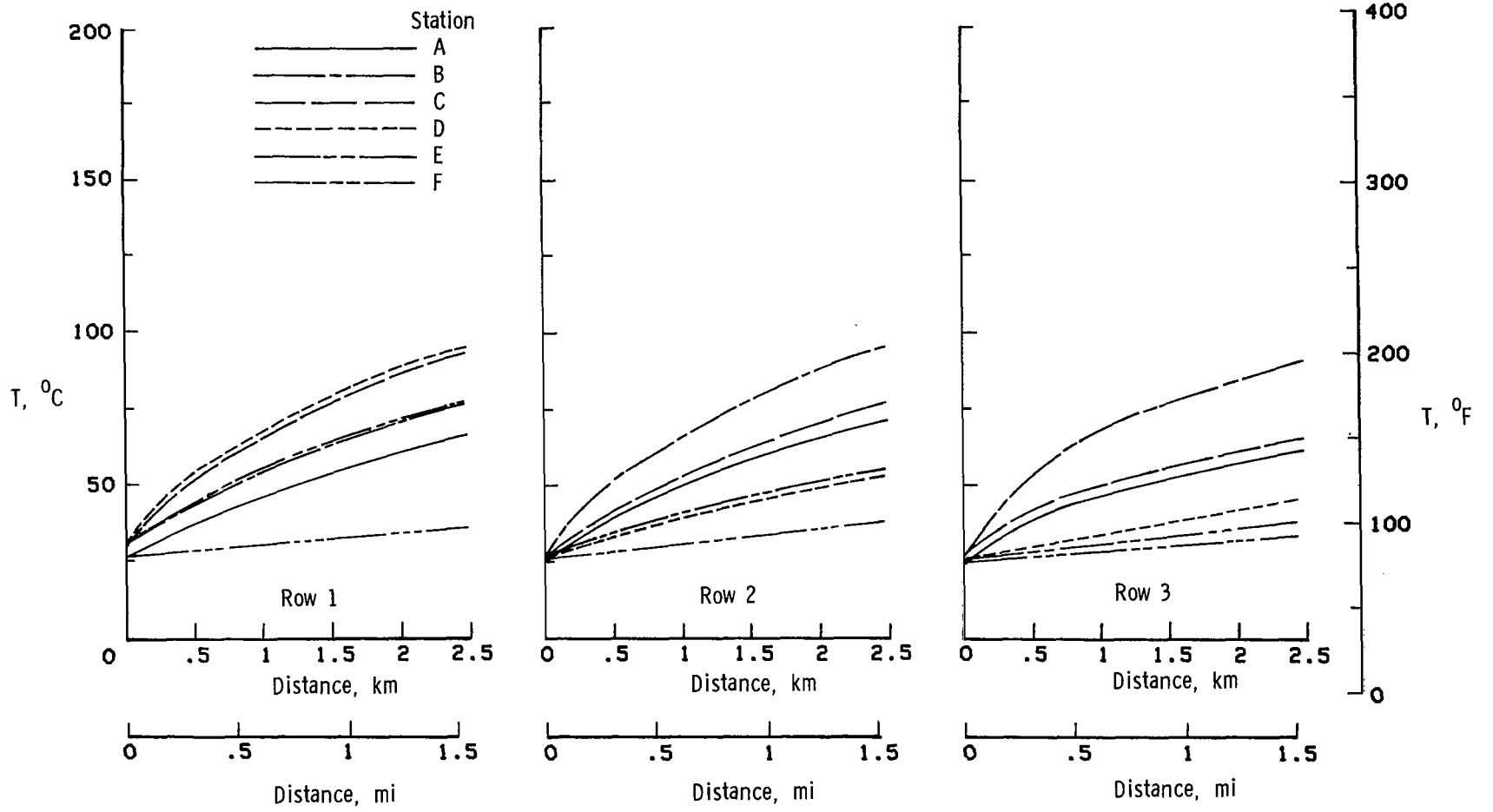
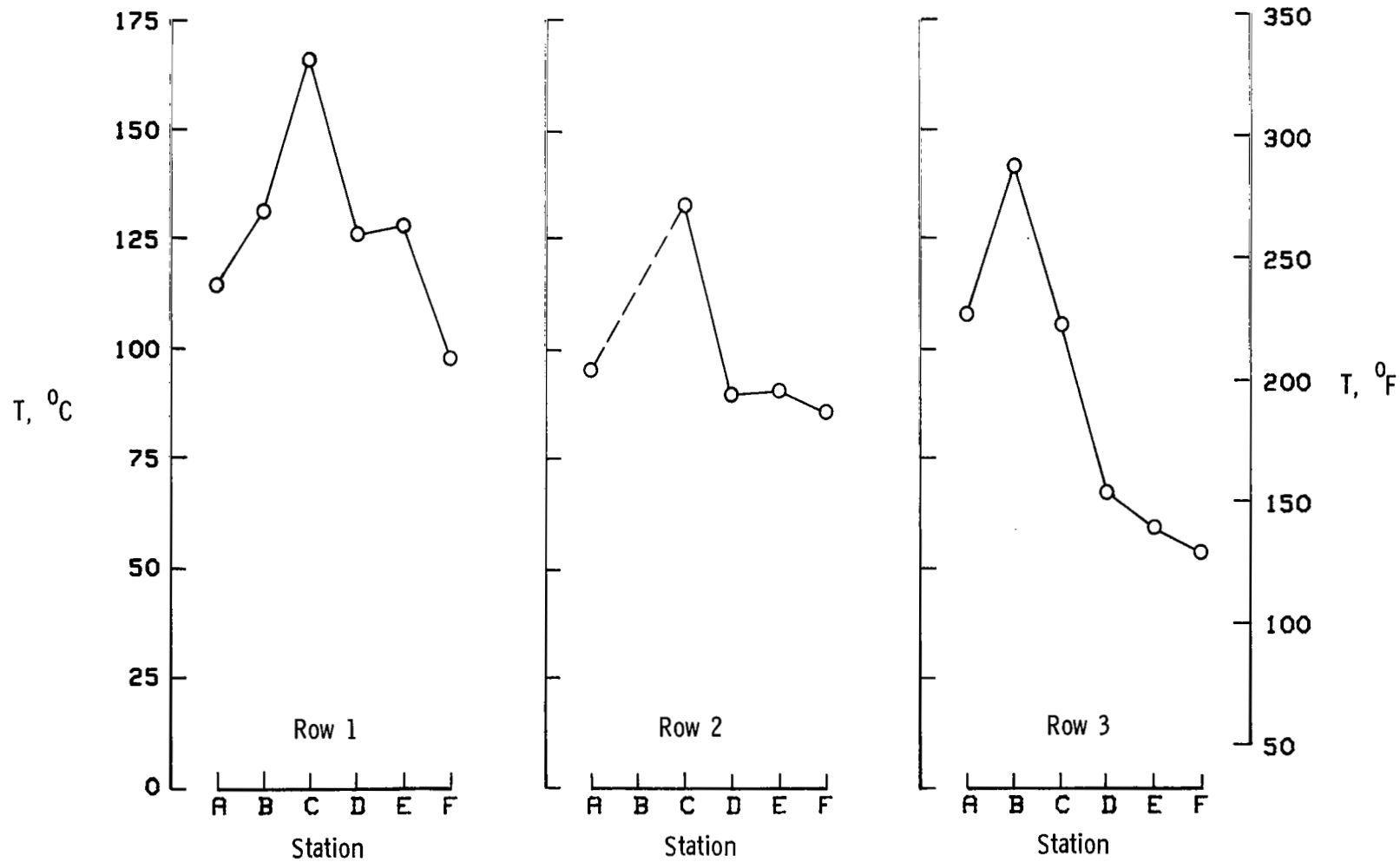


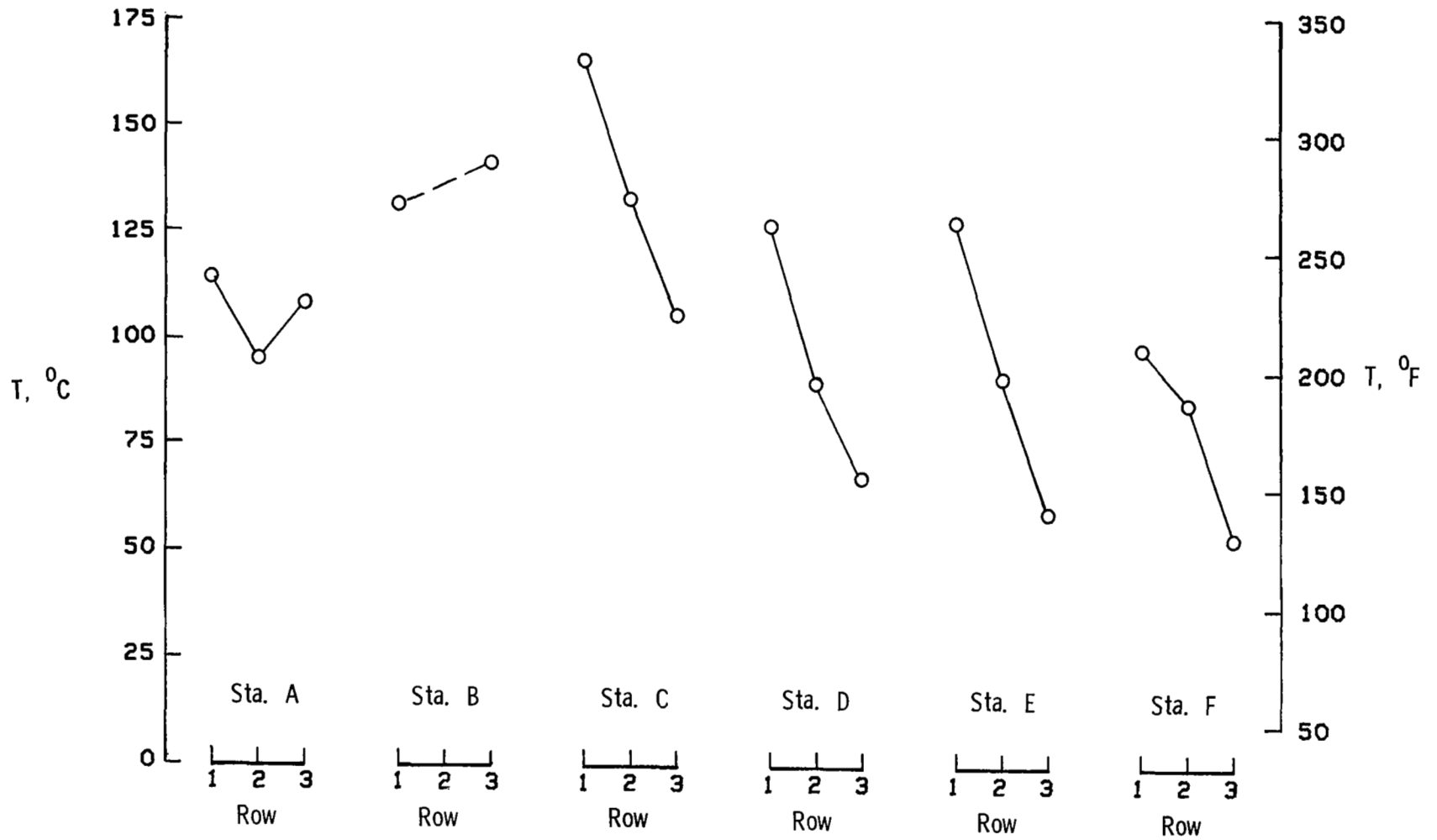
Figure 5.- Temperature buildup with distance traveled for selected test conditions.  $\delta = 30$  percent;  $\psi = 0^\circ$ ; Slip ratio = 0;  $V = 32$  km/hr (20 mph).



(a) Around tire meridian.

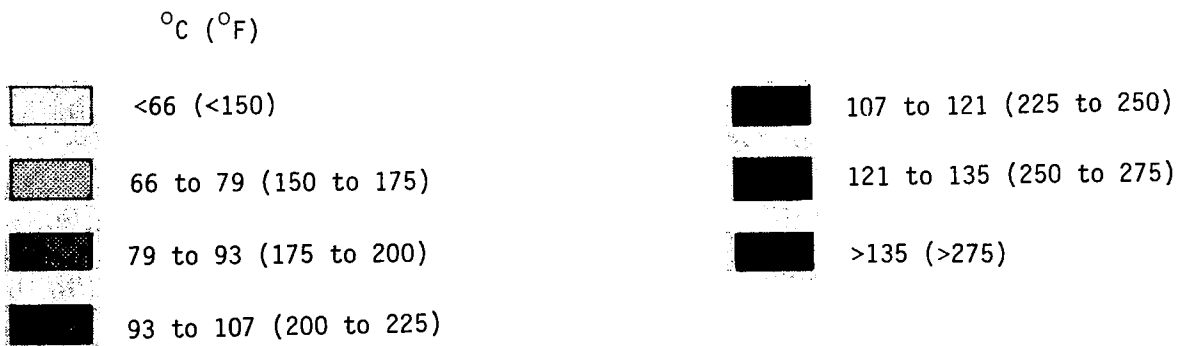
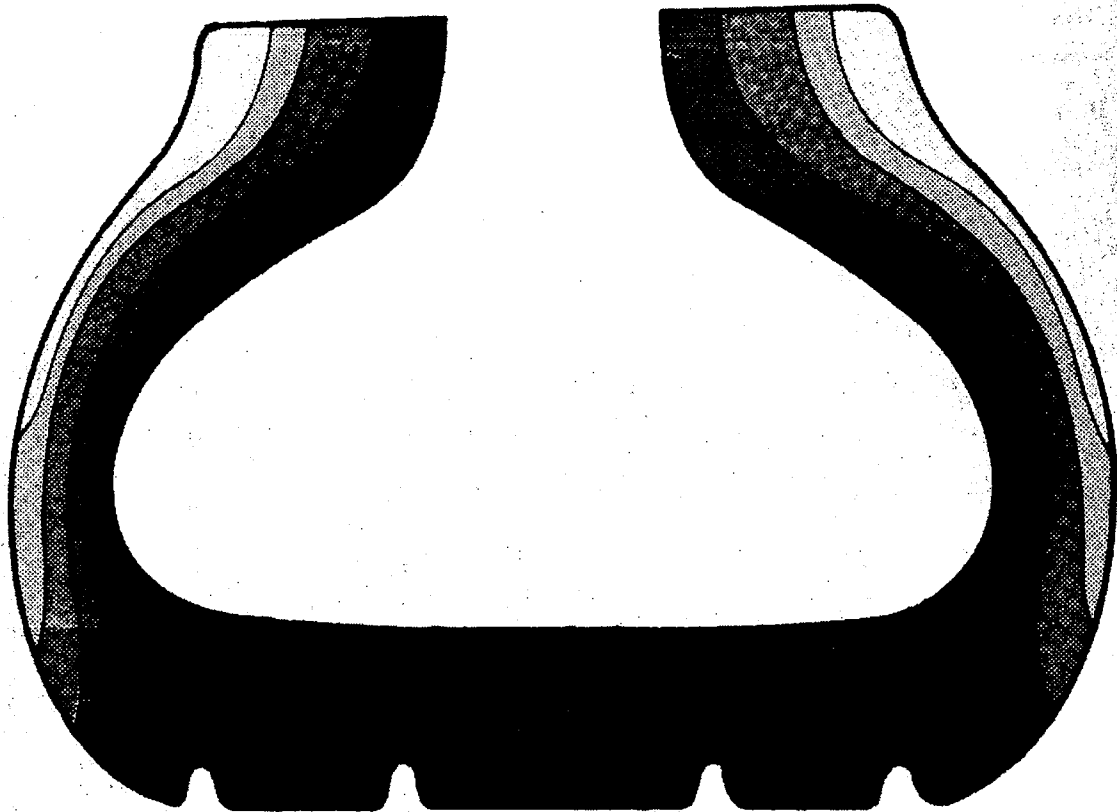
Figure 6.- Tire equilibrium temperature distribution.  $\delta = 30$  percent;  $\psi = 0^\circ$ ; Slip ratio = 0;  $V = 32$  km/hr (20 mph);  $d > 24\ 384$  m (80 000 ft).





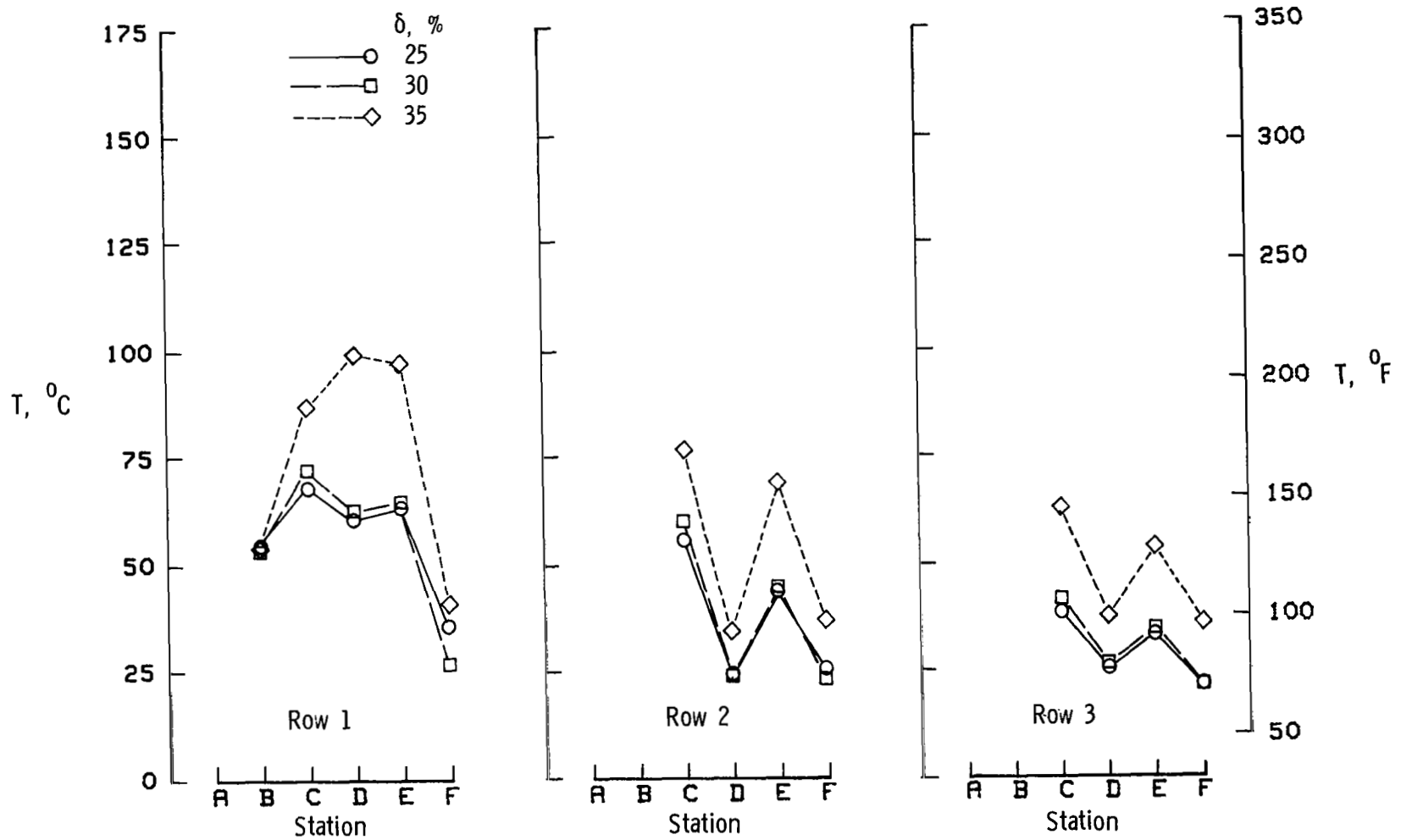
(b) Through tire carcass.

Figure 6.- Continued.



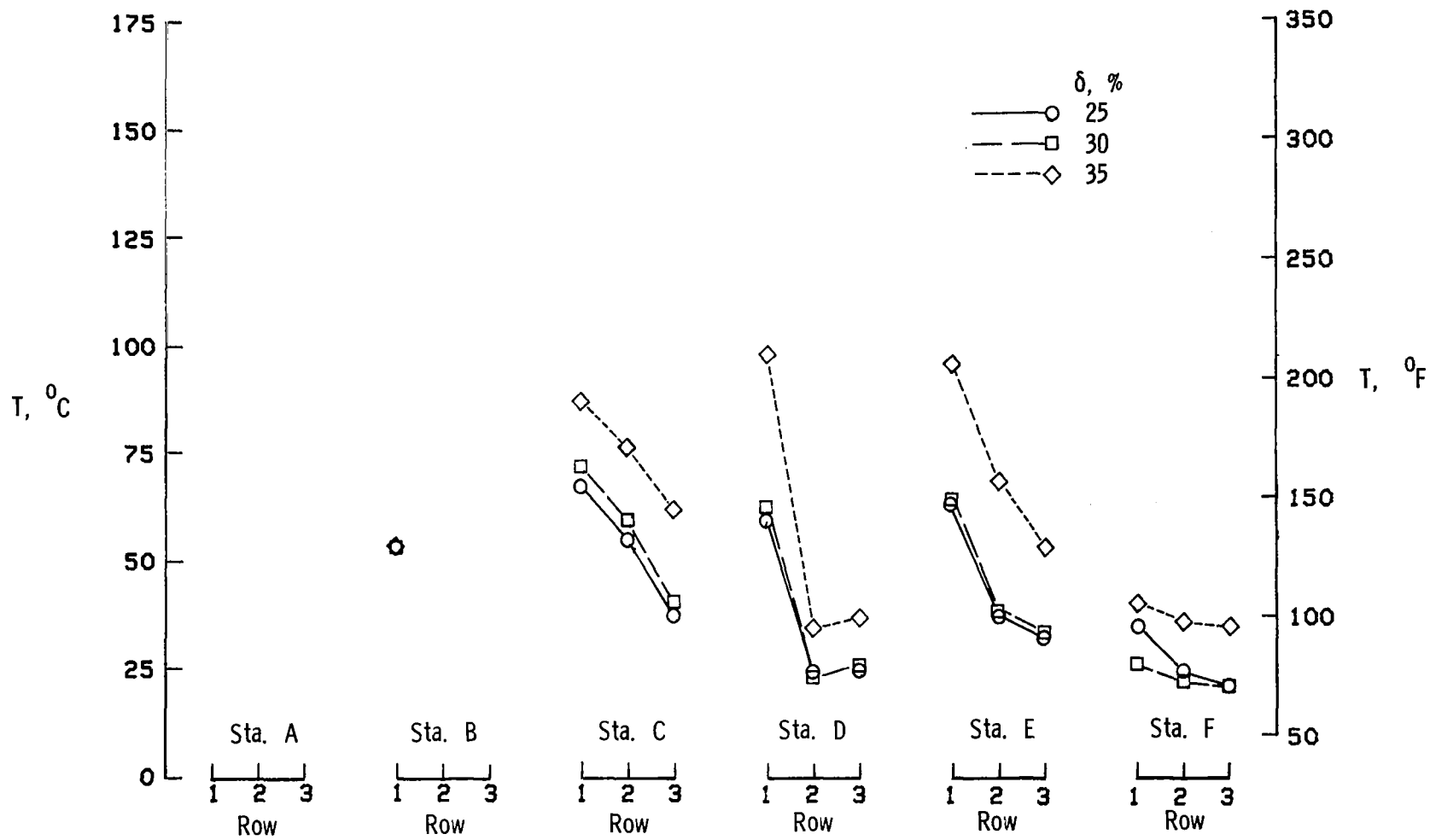
(c) Sketch illustrating complete temperature profile.

Figure 6.- Concluded.



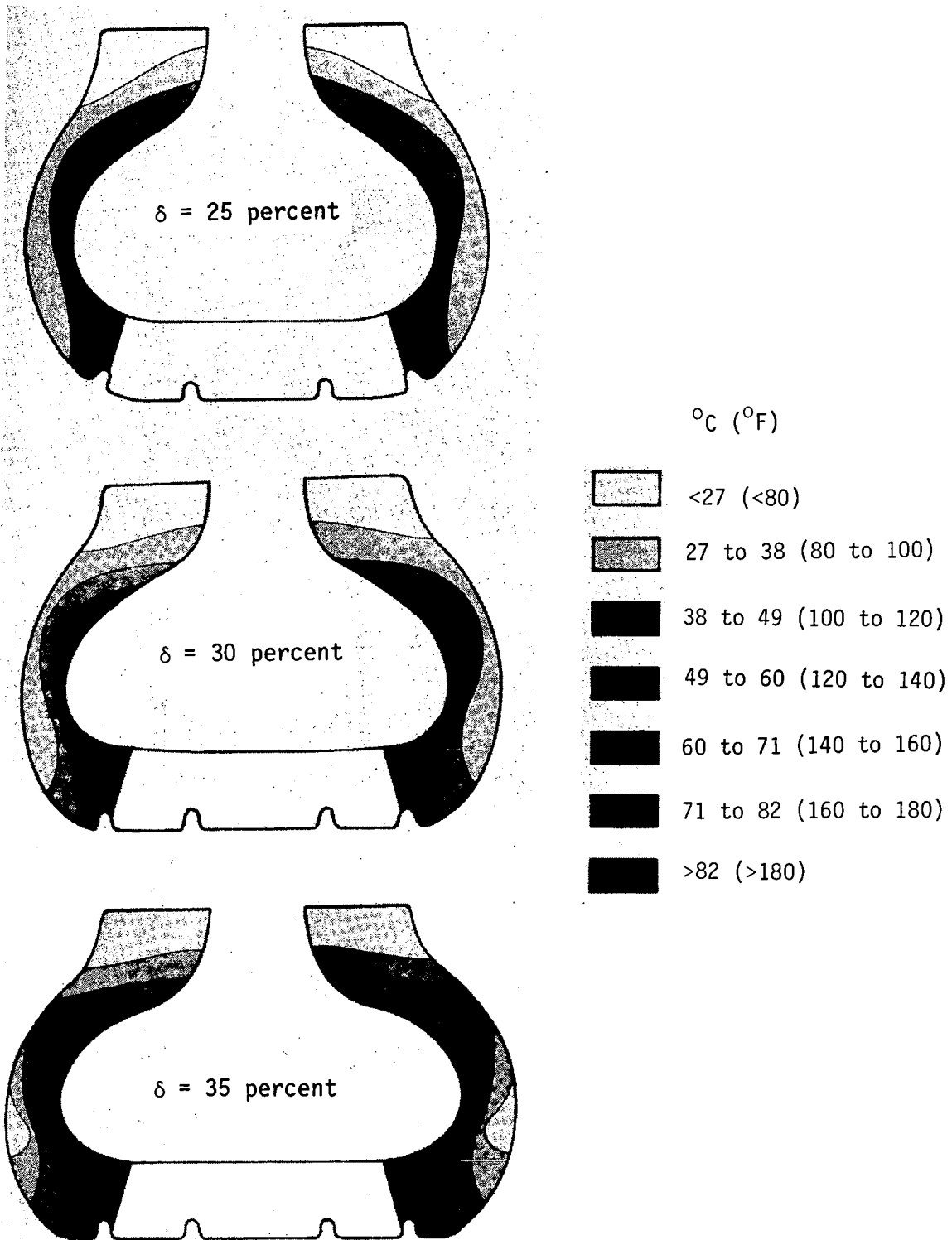
(a) Around tire meridian.

Figure 7.- Effect of tire deflection on temperature distribution in free rolling tire.  $\psi = 0^\circ$ ;  
Slip ratio = 0;  $V = 32$  km/hr (20 mph);  $d = 1524$  m (5000 ft).



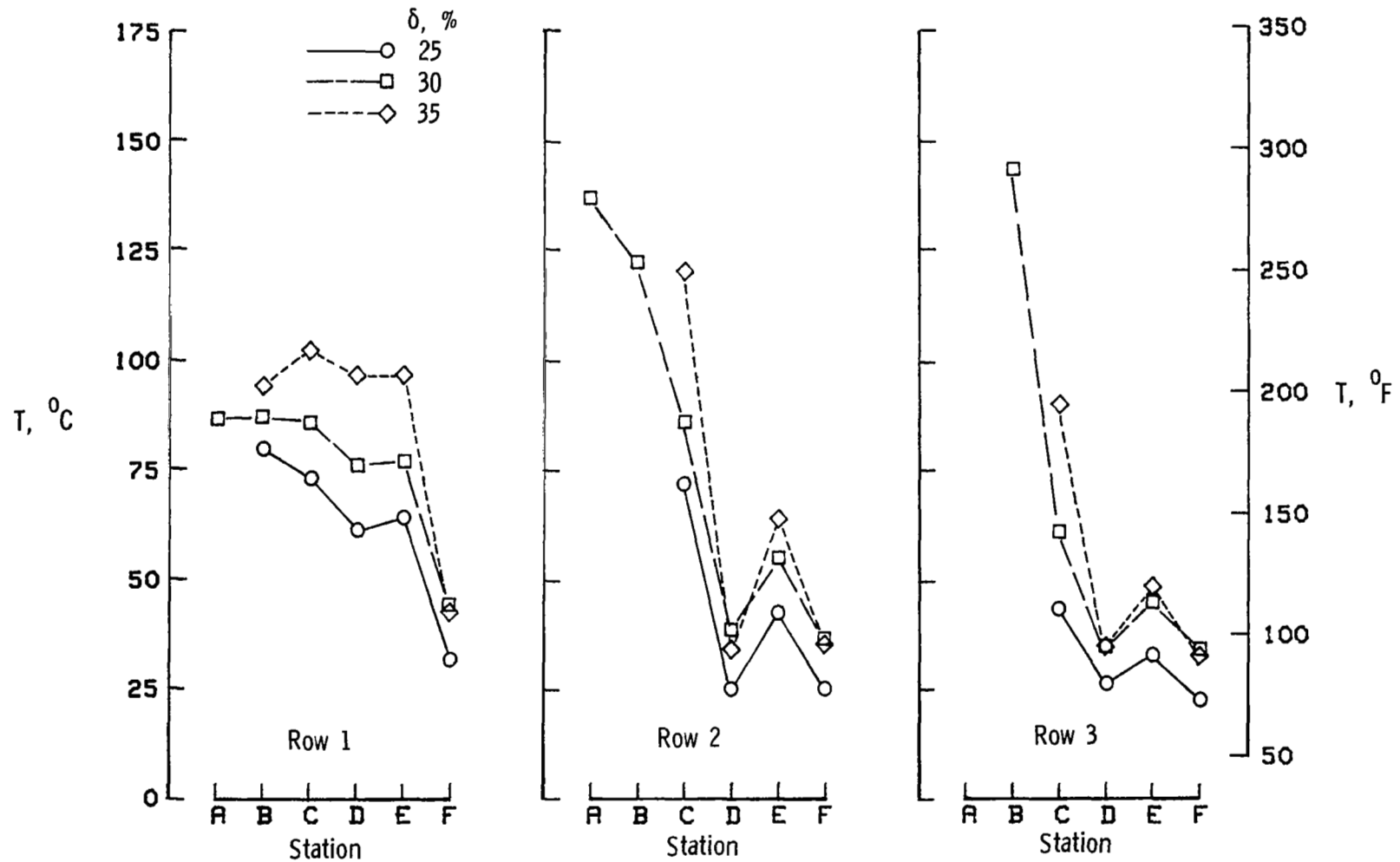
(b) Through tire carcass.

Figure 7.- Continued.



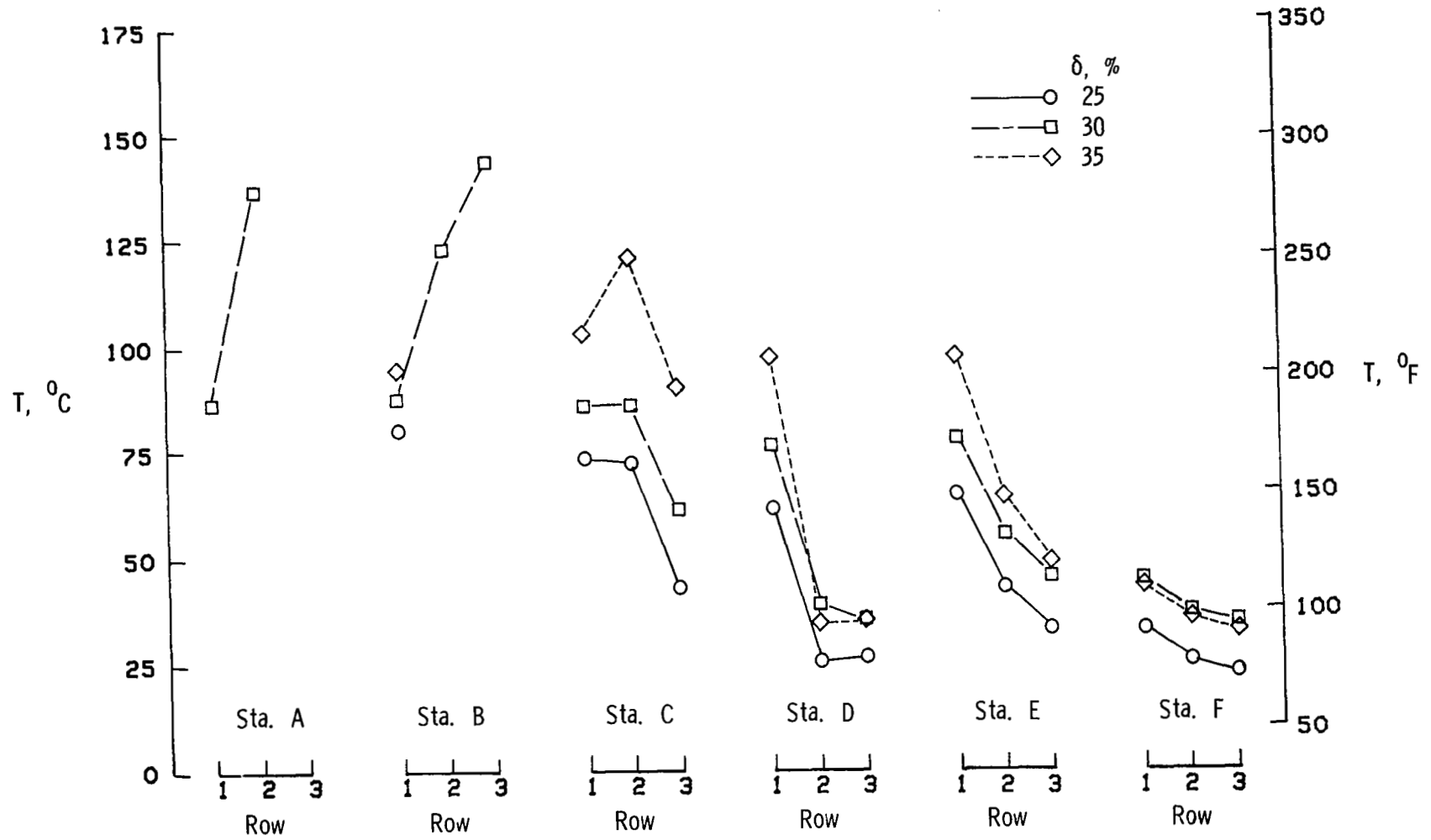
(c) Sketch illustrating complete temperature profile.

Figure 7.- Concluded.



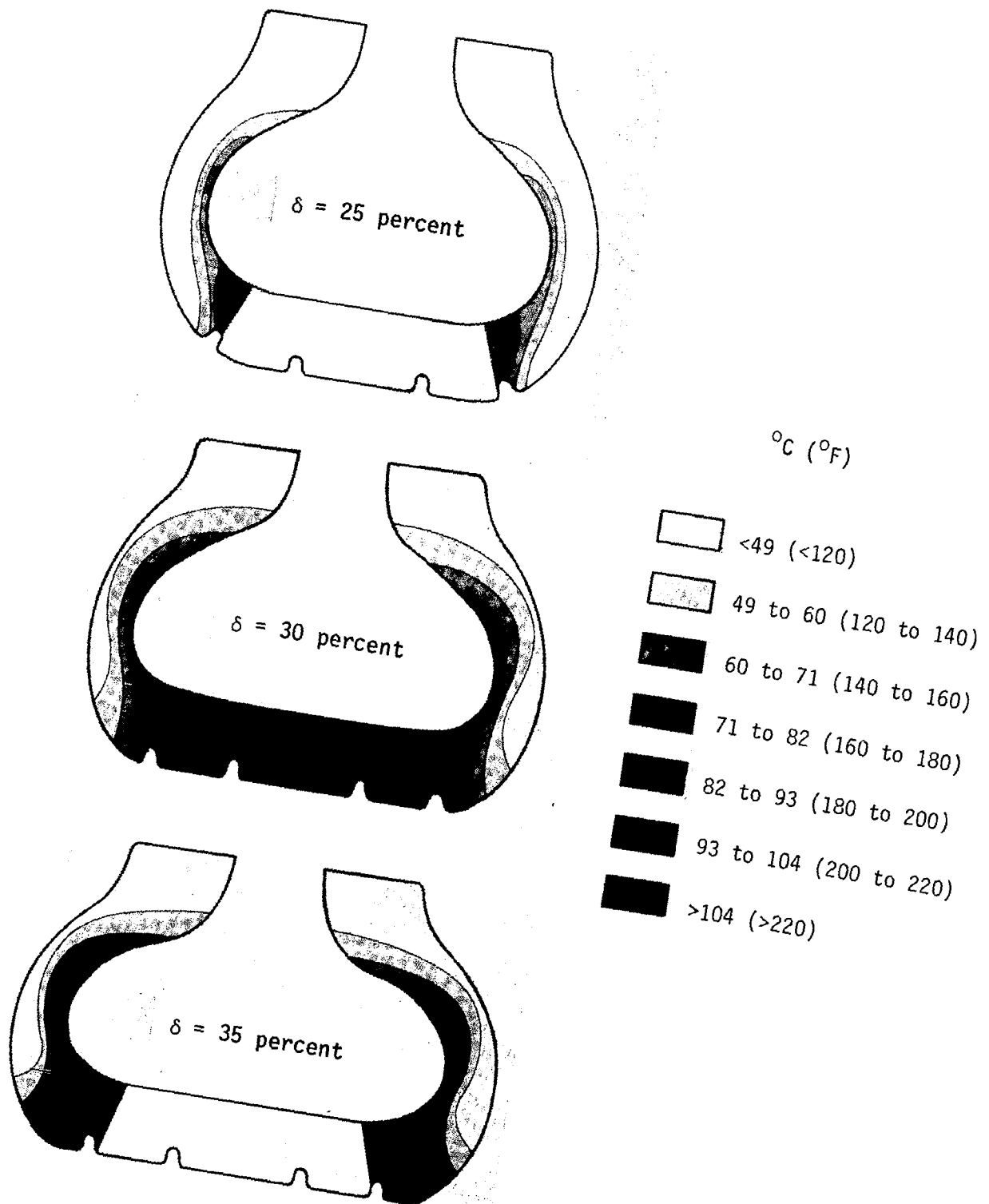
(a) Around tire meridian.

Figure 8.- Effect of tire deflection on temperature distribution in braking tire.  $\psi = 0^\circ$ ; Slip ratio = 0.10;  $V = 32 \text{ km/hr (20 mph)}$ ;  $d = 1524 \text{ m (5000 ft)}$ .



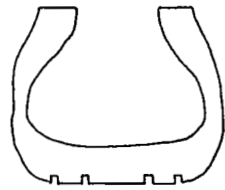
(b) Through tire carcass.

Figure 8.- Continued.



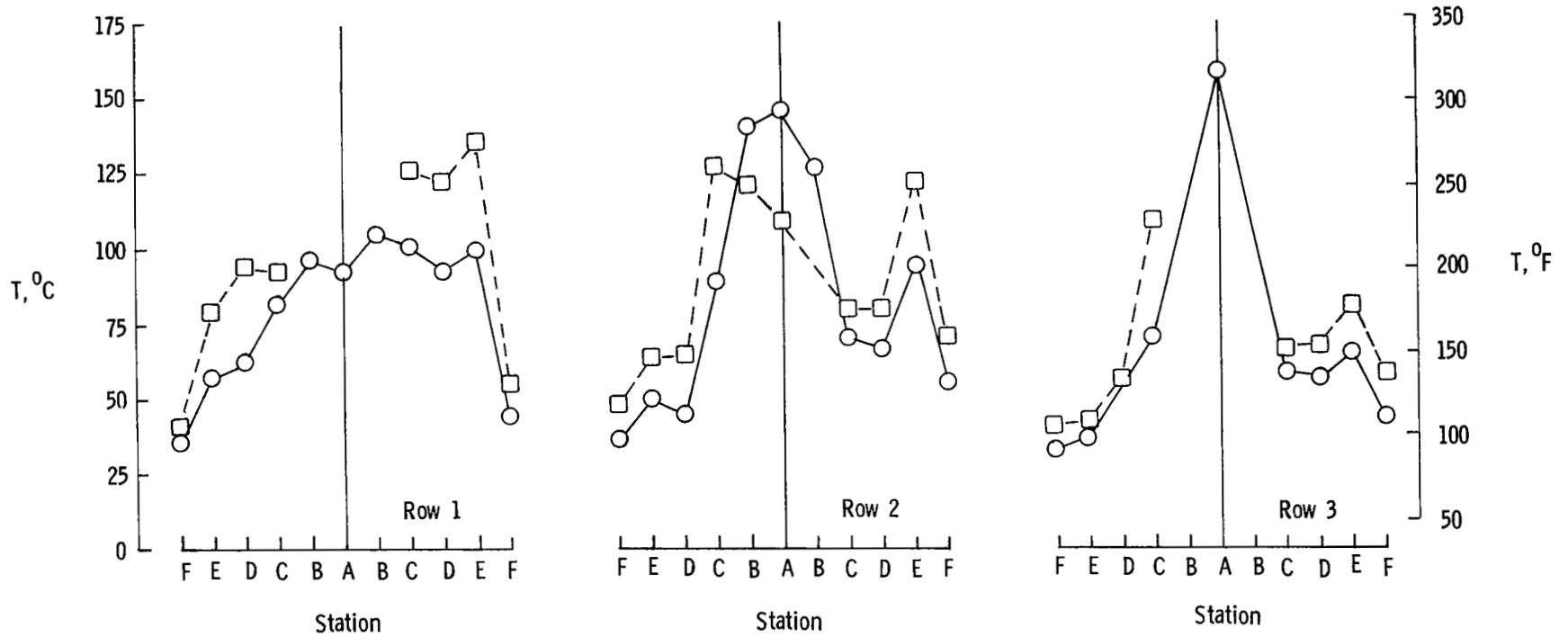
(c) Sketch illustrating complete temperature profile.  
 Figure 8.- Concluded.





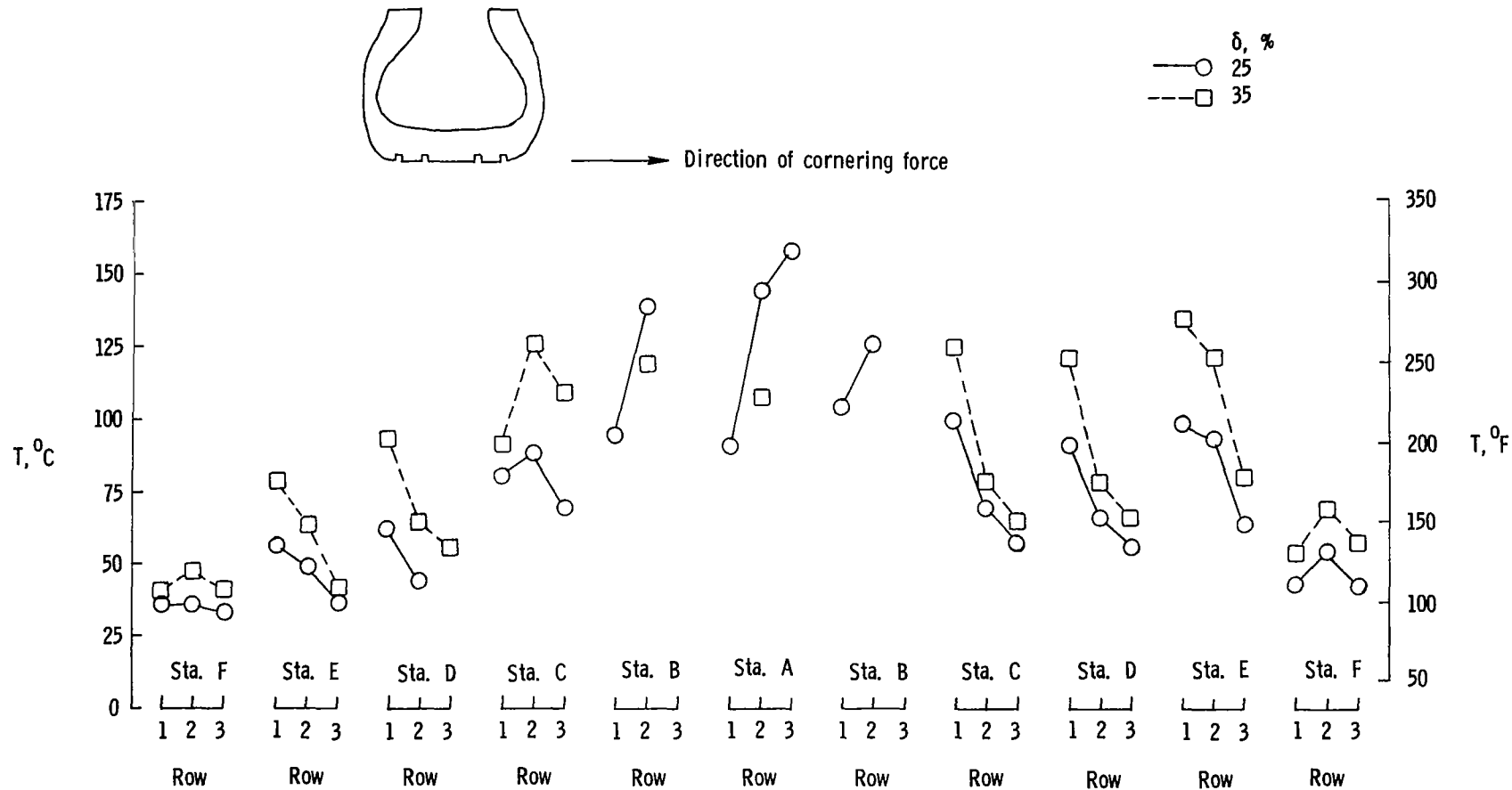
Direction of cornering force

$\delta, \%$   
 —○— 25  
 - -□- 35



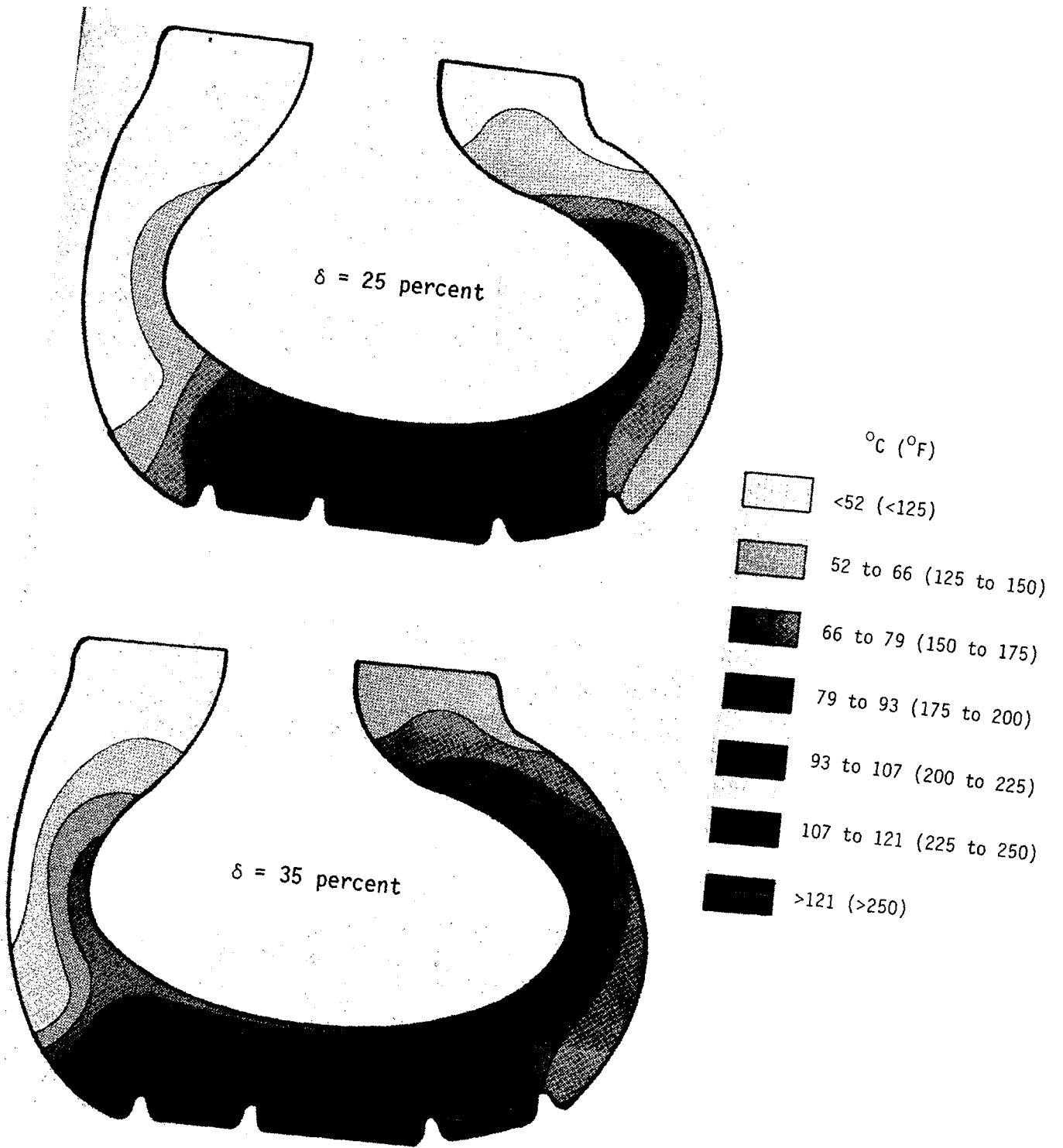
(a) Around tire meridian.

Figure 9.- Effect of tire deflection on temperature distribution in yawed tire.  $\psi = 6^\circ$ ; Slip ratio = 0;  $v = 32 \text{ km/hr (20 mph)}$ ;  $d = 2134 \text{ m (7000 ft)}$ .



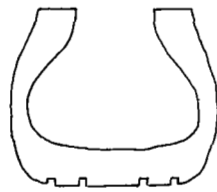
(b) Through tire carcass.

Figure 9.- Continued.

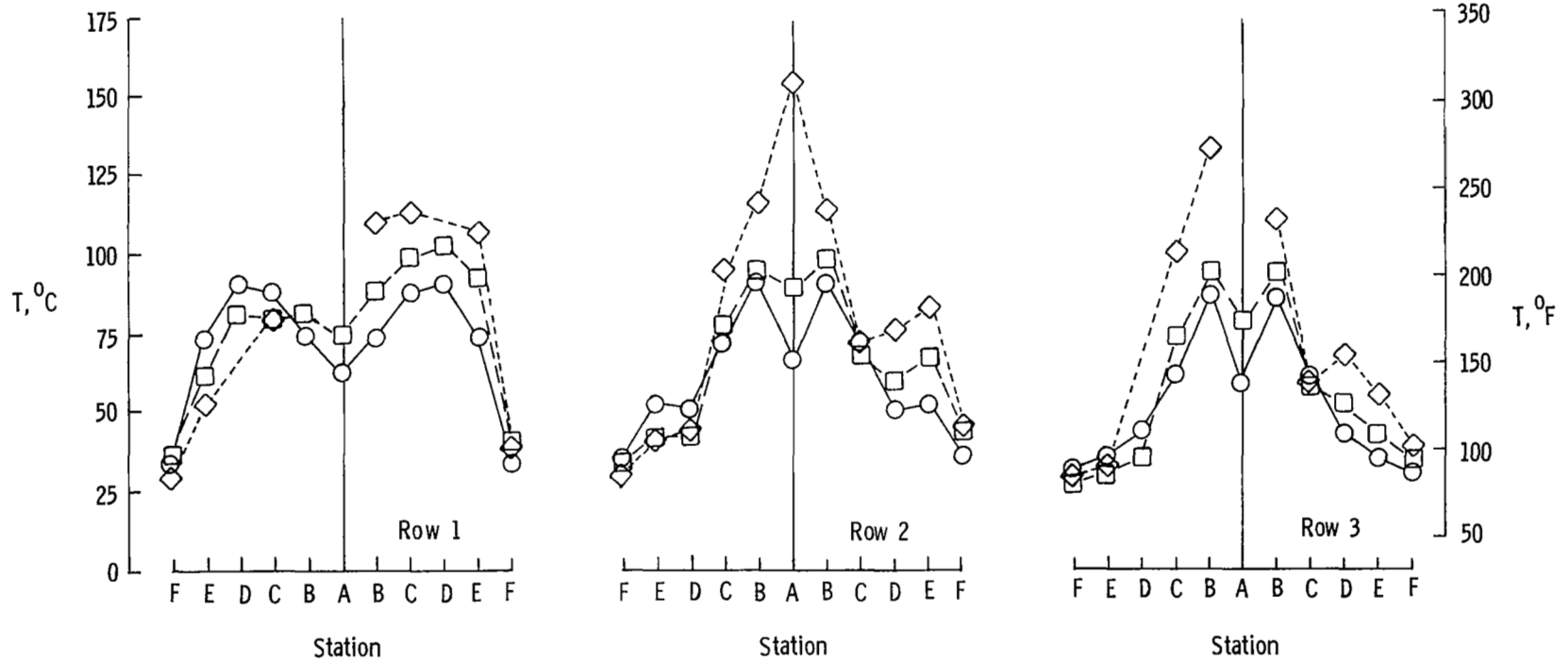
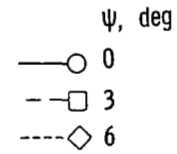


(c) Sketch illustrating complete temperature profile.

Figure 9.- Concluded.

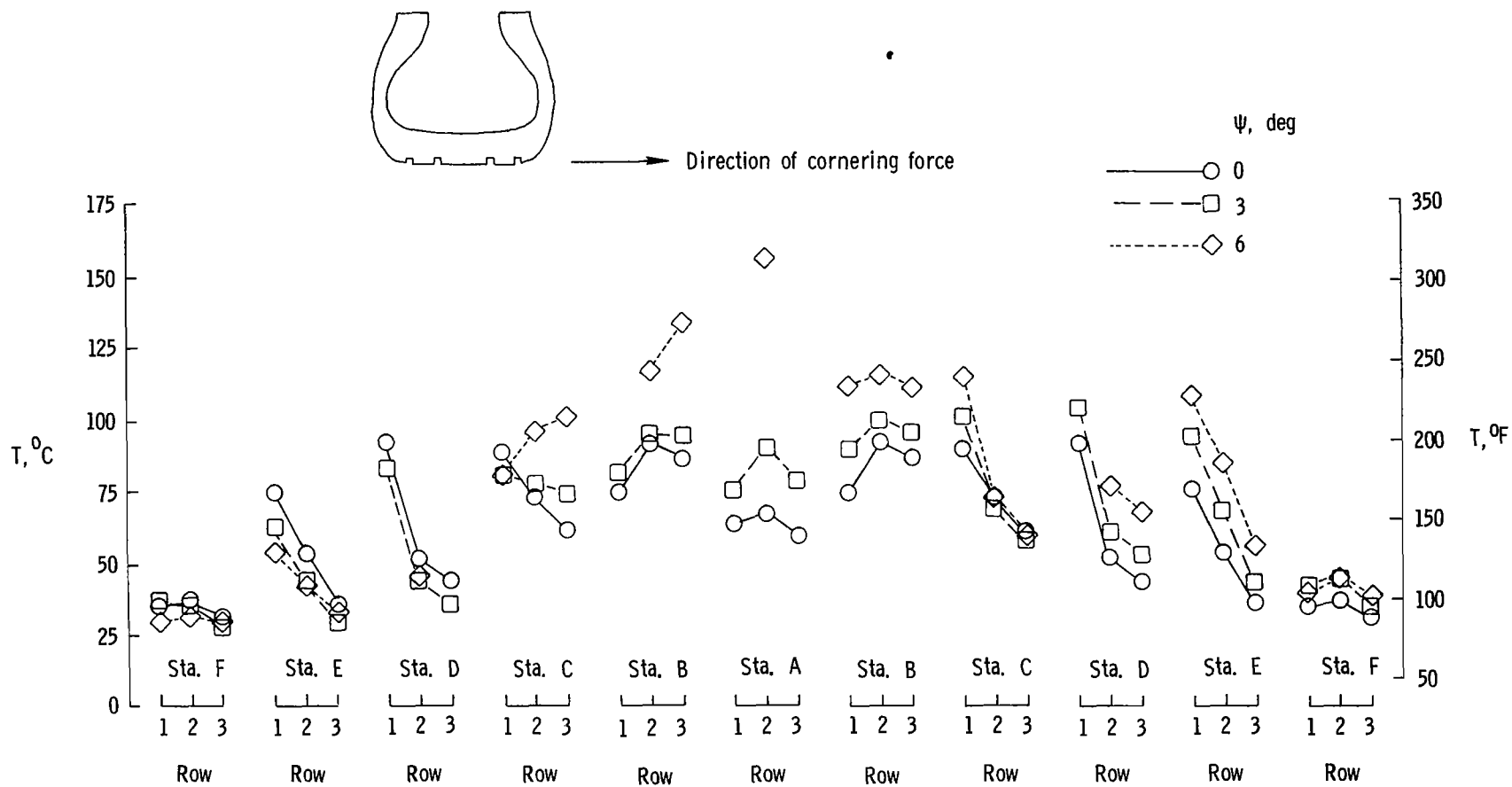


Direction of cornering force



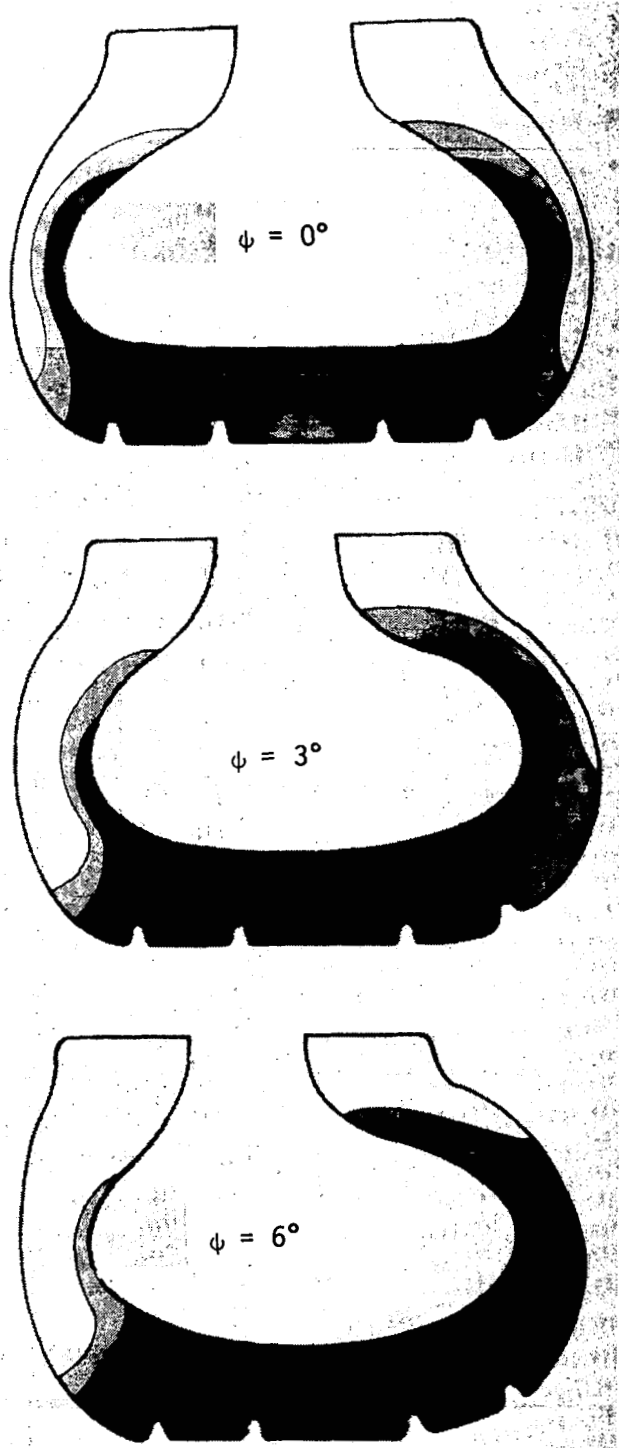
(a) Around tire meridian.

Figure 10.- Effect of yaw angle on tire temperature.  $\delta = 30$  percent; Slip ratio = 0;  $V = 32$  km/hr (20 mph);  $d = 2134$  m (7000 ft).

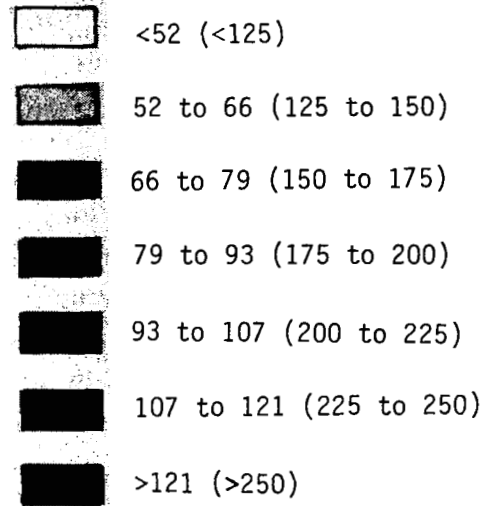


(b) Through tire carcass.

Figure 10.- Continued.

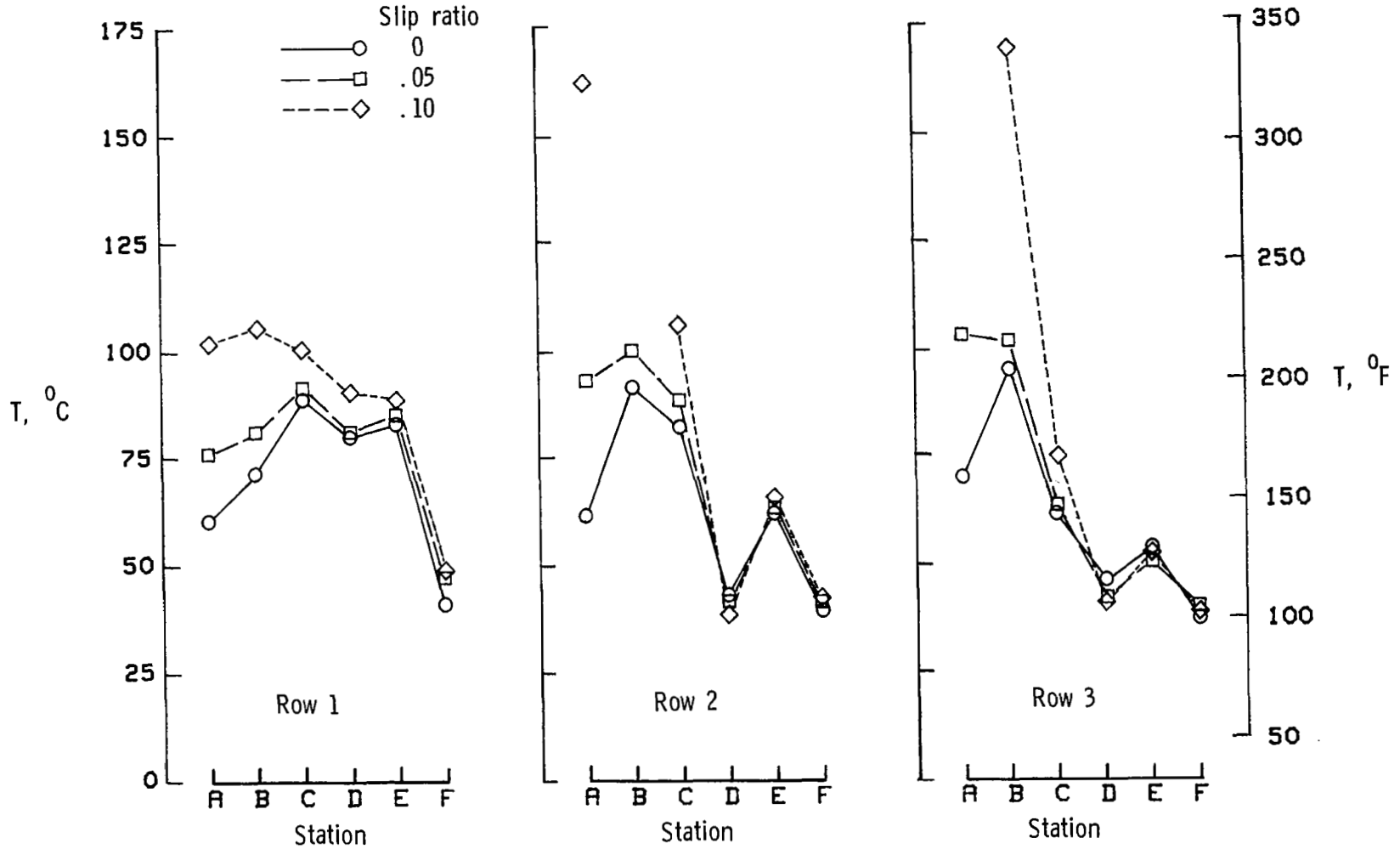


°C (°F)



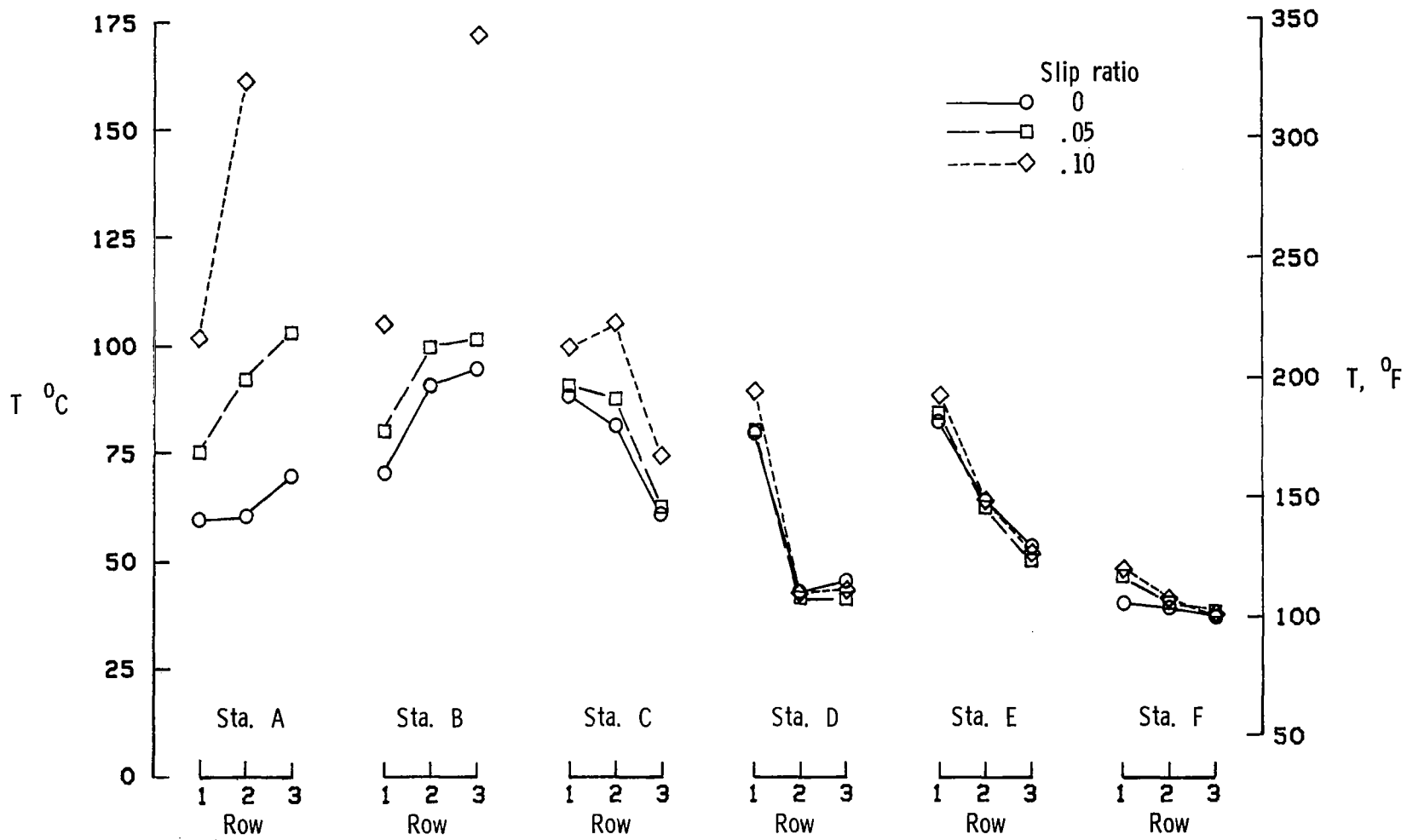
(c) Sketch illustrating complete temperature profile.

Figure 10.- Concluded.



(a) Around tire meridian.

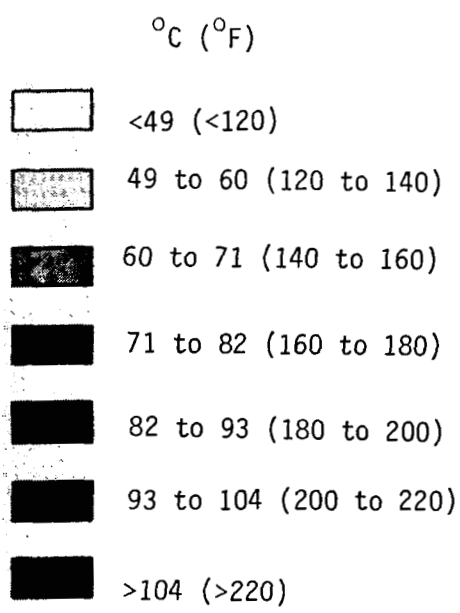
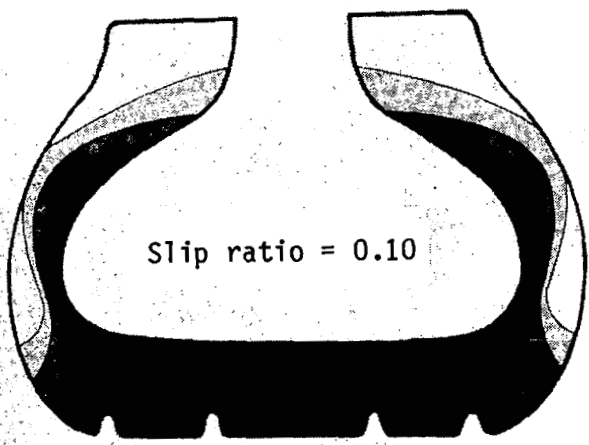
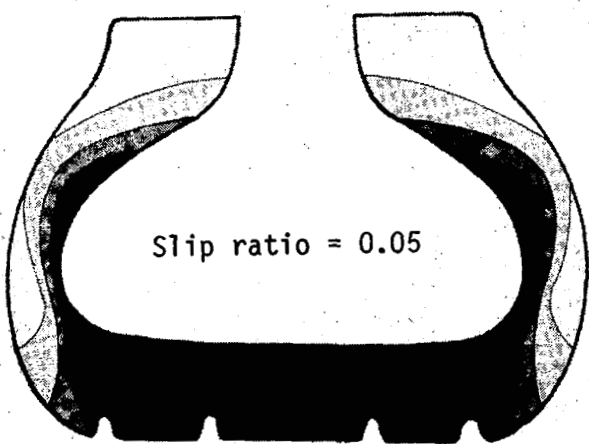
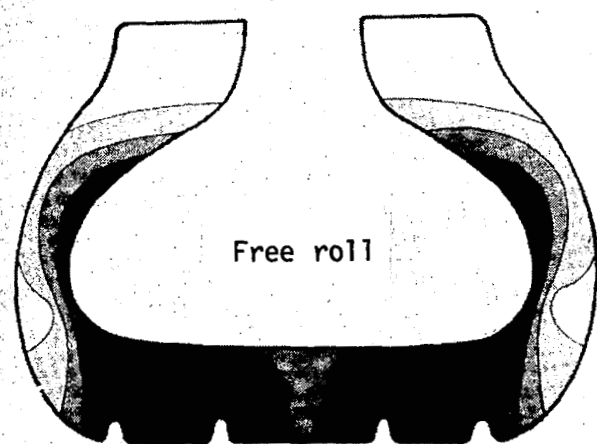
Figure 11.- Effect of slip ratio on tire temperature distribution.  $\delta = 30$  percent;  $\psi = 0^\circ$ ;  $v = 32$  km/hr (20 mph);  $d = 2134$  m (7000 ft).



(b) Through tire carcass.

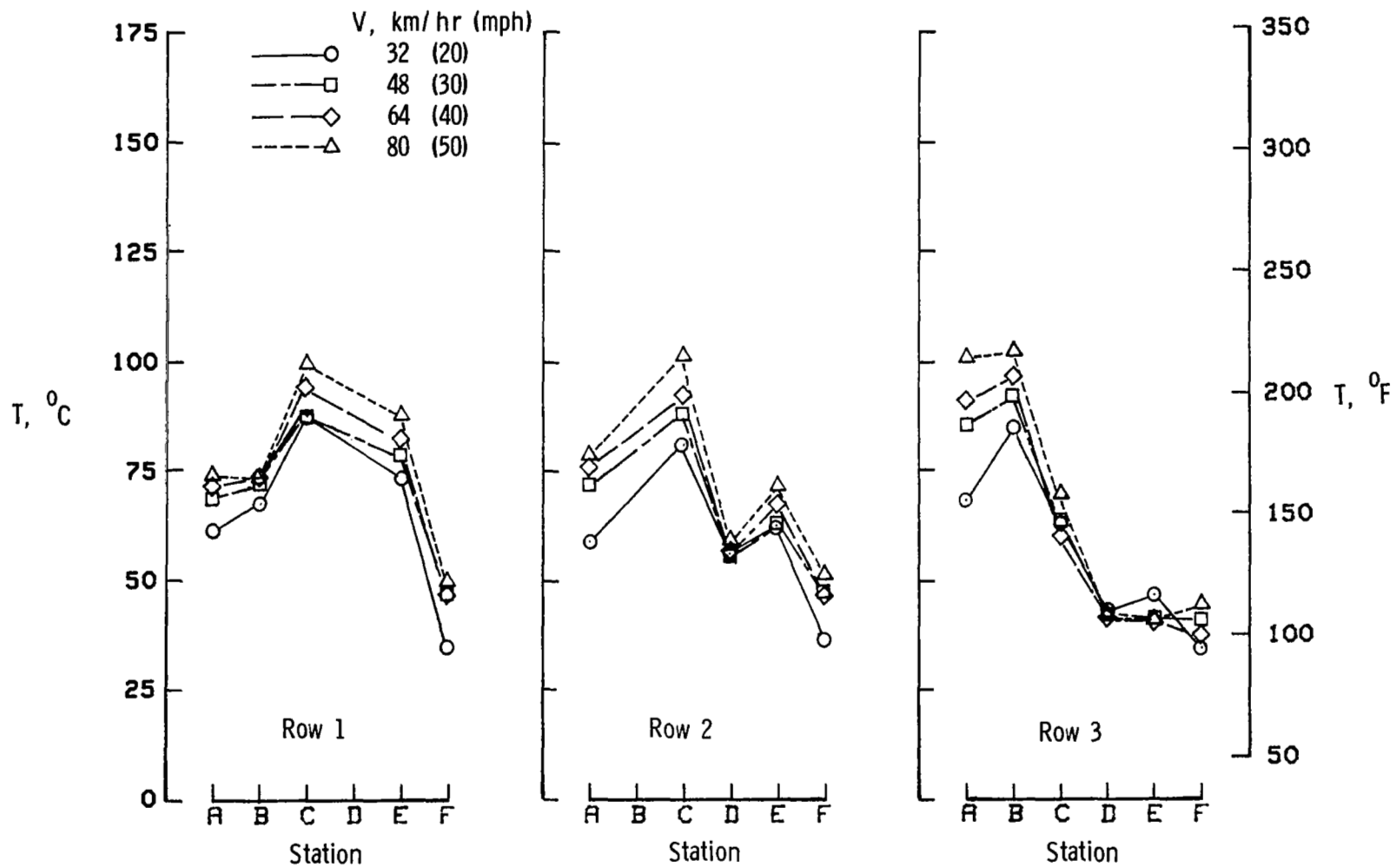
Figure 11.- Continued.





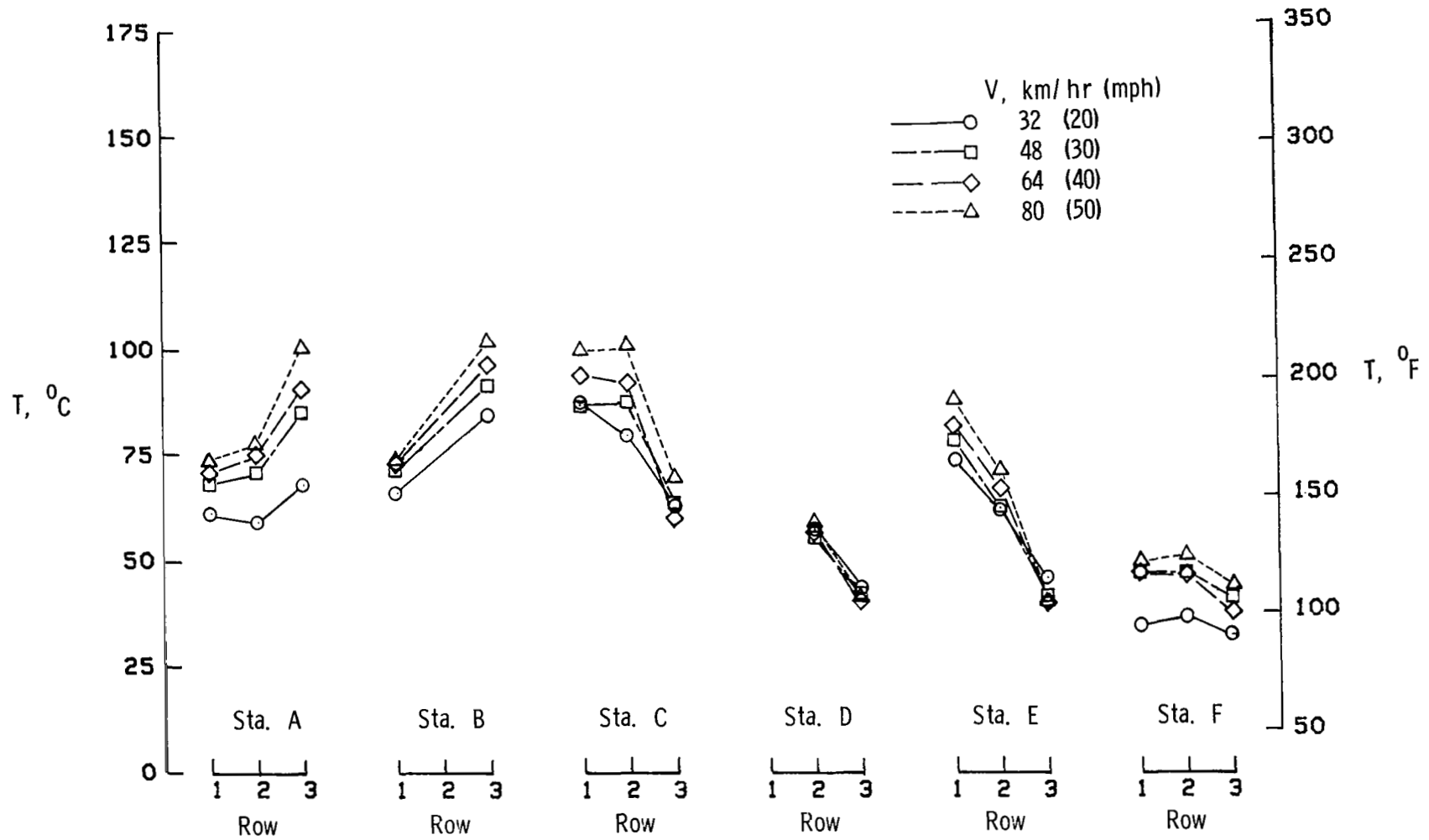
(c) Sketch illustrating complete temperature profile.

Figure 11.- Concluded.



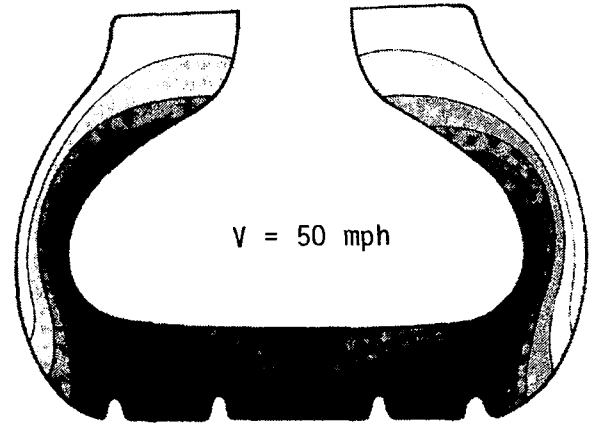
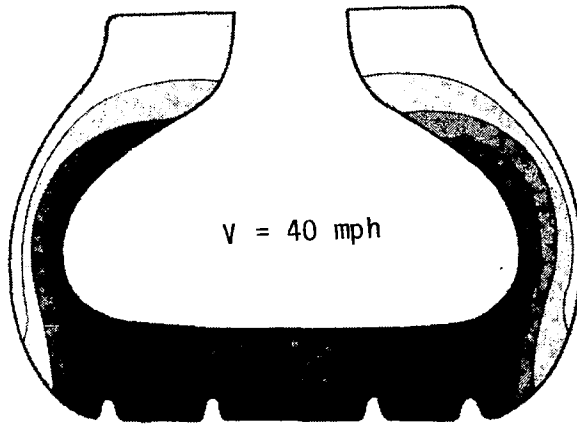
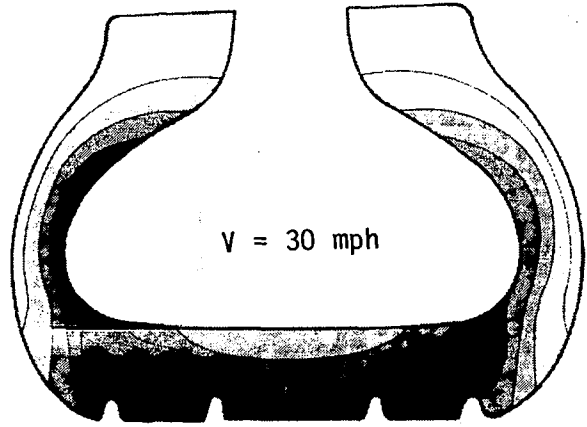
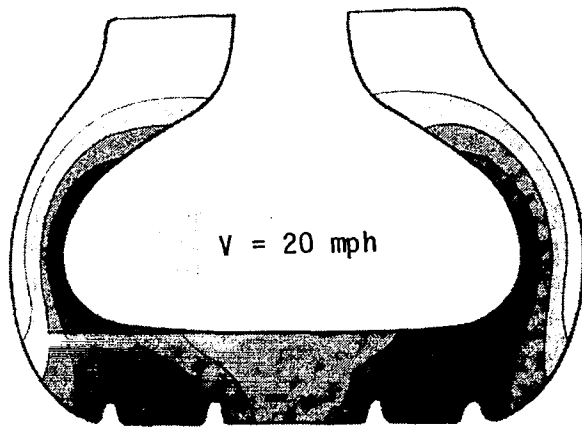
(a) Around tire meridian.

Figure 12.- Effect of speed on temperature distribution in free rolling tire.  $\delta = 30$  percent;  $\psi = 0^\circ$ ; Slip ratio = 0;  $d = 2134$  m (7000 ft).



(b) Through tire carcass.

Figure 12.- Continued.



$^{\circ}\text{C}$  ( $^{\circ}\text{F}$ )

$<49$  ( $<120$ )

$49$  to  $60$  ( $120$  to  $140$ )

$60$  to  $71$  ( $140$  to  $160$ )

$71$  to  $82$  ( $160$  to  $180$ )

$82$  to  $93$  ( $180$  to  $200$ )

$93$  to  $104$  ( $200$  to  $220$ )

$>104$  ( $>220$ )

(c) Sketch illustrating complete temperature profile.

Figure 12.- Concluded.

1. Report No. NASA TP-2195		2. Government Accession No.		3. Recipient's Catalog No.	
4. Title and Subtitle TEMPERATURE DISTRIBUTION IN AN AIRCRAFT TIRE AT LOW GROUND SPEEDS				5. Report Date August 1983	
				6. Performing Organization Code 505-45-23-01	
7. Author(s) John Locke McCarty and John A. Tanner				8. Performing Organization Report No. L-15605	
				10. Work Unit No.	
9. Performing Organization Name and Address NASA Langley Research Center Hampton, VA 23665				11. Contract or Grant No.	
				13. Type of Report and Period Covered Technical Paper	
12. Sponsoring Agency Name and Address National Aeronautics and Space Administration Washington, DC 20546				14. Sponsoring Agency Code	
15. Supplementary Notes					
16. Abstract  An experimental study was conducted to define temperature profiles of 22 x 5.5, type VII, bias ply aircraft tires subjected to freely rolling, yawed rolling, and light braking conditions. Temperatures along the inner wall of freely rolling tires were greater than those near the outer surface. The effect of increasing tire deflection was to increase the temperature within the shoulder and sidewall areas of the tire carcass. The effect of cornering and braking was to increase the tread temperature. For taxi operations at fixed yaw angles, temperature profiles were not symmetric. Increasing the ground speed produced only moderate increases in tread temperature, whereas temperatures in the carcass shoulder and sidewall were essentially unaffected.					
17. Key Words (Suggested by Author(s)) Aircraft tires Carcass temperatures Free rolling Yawed rolling Light braking			18. Distribution Statement Unclassified - Unlimited  Subject Category 39		
19. Security Classif. (of this report) Unclassified		20. Security Classif. (of this page) Unclassified		21. No. of Pages 34	22. Price A03